DEPARTMENT OF OCEAN ENGINEERING

MASSACHUSETTS INSTITUTE OF TECHNOLOGY

CAMBRIDGE, MASSACHUSETTS 02139

PREDICTED HEAT TRANSFER LOSS IN THE EXPANSION CYLINDER OF A TWO CYLINDER RECIPROCATING ENGINE

by

Paul Christian Jorgensen

Course XIII-A

SM (NAME)

SM (ME)

May 1984

PREDICTED HEAT TRANSFER LOSS IN THE EXPANSION CYLINDER OF A TWO CYLINDER CYCLE RECIPROCATING ENGINE

by

PAUL CHRISTIAN JORGENSEN

B.S., UNITED STATES NAVAL ACADEMY
(1972)

Submitted to the Department of Ocean Engineering
in partial fulfillment of the
Requirements of the Degrees of

MASTER OF SCIENCE IN NAVAL ARCHITECTURE AND MARINE ENGINEERING

and

MASTER OF SCIENCE IN MECHANICAL ENGINEERING

at the

MASSACHUSETTS INSTITUTE OF TECHNOLOGY

May 1984

PREDICTED HEAT TRANSFER LOSS IN THE EXPANSION CYLINDER OF A TWO CYLINDER CYCLE RECIPROCATING ENGINE

by

PAUL CHRISTIAN JORGENSEN

Submitted to the Department of Ocean Engineering on 11 May, 1984 in partial fulfillment of the requirements for the Degrees of Master of Science in Naval Architecture and Marine Engineering and Master of Science in Mechanical Engineering.

ABSTRACT

Carmichael [1] has proposed a direct injection, temperature ignition (TI), reciprocating engine design which divides the conventional four stroke cycle functions between a compression cylinder and an expansion cylinder, interconnected by a static regenerative heat exchanger. The prediction of heat transfer loss in the expansion cylinder is required to predict the performance of the new cycle.

Woschni's correlations [9], developed for direct injection, quiescent, four stroke, compression ignition (CI) engines, are used to predict uncorrected expansion cylinder heat transfer loss. Laws of similarity allow, in principle, extrapolation outside the experimental data range for forced convection heat transfer only. General applicability of Woschni's correlations is established by examining the expansion cylinder quiescent condition, using predicted mean gas velocity magnitudes and fully developed, turbulent flow, forced convection models. Predicted radiant peak flame emissivity and temperature are found and compared with nominal peak values observed in conventional CI engine cycles to establish a minimum radiation flux reduction ratio. A mean reduction ratio for forced convection flux is also found. A corrected, conservative prediction of heat transfer loss in the expansion cylinder is then established.

Thesis Supervisor: A. Douglas Carmichael
Title: Professor of Power Engineering

ACKNOWLEDGEMENTS

I would like to extend my deepest appreciation to Professor A. Douglas Carmichael and Assistant Professor Wai K. Cheng for their instruction and guidance both in preparation of this thesis and in the classroom during my formal education at M.I.T.. I would additionally like to thank Professor J. B. Heywood for his kind assistance and timely comments.

I would like to thank Richard and Irene Martin for the production of this thesis on their home computerized printing press.

I would especially like to thank my wife, Janis, and our children, Mark, Kate, and Karin. Their understanding, faith, and love have been a constant support through our two years at M.I.T..

TABLE OF CONTENTS

TABLE OF CONTENTS (CONT)

TABLE OF CONTENTS (CONT)

NOMENCLATURE

Alphanumeric

A	heat transfer surface area [ft^2]
A_{HT}	cylinder heat transfer surface area [ft^2]
A_p	regenerator port exit cross-sectional area [ft^2]
a	crank radius length [ft]
B	bore diameter [ft]
B_e	fuel consumption rate [lbm/hr]
Bo	Boltzmann number; defined by equation (61)
C_f	friction coefficient; defined by equation (11)
C_p	specific heat at constant pressure [BTU/lbm-°R]
C_v	specific heat at constant volume [BTU/lbm-°R]
C_1 & C_2	Woschni correlation constants; defined by equations 18a - 18e
c	speed of light = 2.997902×10^{10} cm/sec
c_b	Boltzmann's constant = 1.38026×10^{-16} erg/°K
c_p	Planck's constant = 6.623777×10^{-27} erg-sec
c_s	soot formation rate coefficient [$lbm/sec-ft^3-atm$]
D	diameter [ft]
E	radiant emissive power [$BTU/hr-ft^2$ or $BTU/sec-ft^2$]
E_λ	radiant monochromatic emissive power [$ergs/sec-cm^2-\lambda(cm)$]
E_s	soot combustion activation energy [BTU/mole(lbm)]
F	radiant geometric view factor
h	heat transfer coefficient [$BTU/hr-ft^2-°R$]

h_D	heat transfer coefficient across pipe diameter D; turbulent flow [BTU/hr-ft^2-°R]
h_e	total cylinder heat transfer coefficient; turbulent flow [BTU/hr-ft^2-°R]
h_l	heat transfer coefficient across length l of flat plate; turbulent flow [BTU/hr-ft^2-°R]
h_x	local heat transfer coefficient at distance x from leading edge of flat plate; turbulent flow [BTU/hr-ft^2-°R]
j	Colburn factor; defined by equation (9)
K	thermal conductivity [BTU/hr-ft-°R]
k_f	apparent flame absorption coefficient per unit length [ft^{-1}]
k_g	apparent gas absorption coefficient per unit length [ft^{-1}]
k_p	apparent flame absorption coefficient per unit length-unit pressure [ft-atm]$^{-1}$
k_λ	monochromatic absorption coefficient per unit length [ft-λ]$^{-1}$
L	piston stoke [ft]
L_θ	cylinder gas volume height [ft]
$\mathfrak{L}$	flame luminosity
l	flat plate length [ft]
l_c	Re characteristic length [ft]
l_R	effective radiant mean beam length [ft]
l_r	connecting rod length [ft]
m	charge mass [lbm]
m_c	charge mass at ignition start [lbm]
$\dot{m}$	charge mass flow rate [lbm/sec]
N_{RPM}	cylinder cycle frequency [RPM]
Nu	Nusselt number; defined by equation (3)
P	cylinder pressure [atm]

P_c	cylinder pressure at ignition start [atm]
P_o	cylinder motoring pressure [atm]
Pr	Prandtl number; defined by equation (5)
P_u	unburnt fuel partial pressure in the soot formation zone [atm]
Q	heat transfer [BTU]
$\dot{Q}$	heat transfer rate [BTU/sec]
q	heat transfer flux [BTU/sec-ft^2]
q_λ	monochromatic radiant heat transfer flux [BTU/sec-ft^2-λ]
R_c	crank ratio = l_r/a
R_o	universal gas constant [BTU/mole(lbm)-°R]
R	specific gas constant = 53.90 lbf-ft/lbm-°R
Re	Reynolds number; defined by equation (4)
Re_D	Reynolds number for pipe flow; l_c = D
Re_x	local Reynolds number for flat plate at distance x; l_c = x
r_c	cylinder compression ratio
S_p	piston speed [ft/sec]
$\mathcal{S}$	soot concentration [lbm/ft^3]
SFC	specific fuel consumption [lbm fuel/HP-hr]
St	Stanton number; defined by equation (10)
s	straight line distance between cylinder crank shaft and piston pin [ft]
T	temperature [°R]
Tg	cylinder bulk gas temperature [°R]
Tg_c	cylinder bulk gas temperature at ignition start [°R]
T_o	cylinder motoring bulk gas temperature [°R]

T_u	local temperature of the soot formation zone [°R]
Tw	heat transfer surface wall temperature [°R]
t	unit time [sec]
V	cylinder gas volume [ft^3]
Vc	cylinder clearance volume at piston TDC [ft^3]
V_c	cylinder volume at ignition start (ft^3)
V_u	volume of the soot formation zone [ft^3]
U	bulk fluid (gas) velocity [ft/sec]
Ui	impulse charge velocity exiting regenerator port [ft/sec]
Uexp	bulk gas velocity at the cylinder walls in the expansion stroke [ft/sec]
Uexh	bulk gas velocity at the cylinder walls in the exhaust stroke [ft/sec]
ω_r	angular gas velocity at radius r [ft/sec]
X	radiant path length [ft]

Symbols

Φ	charge equivalence ratio
Φ_u	unburnt fuel equivalence ratio in the soot formation zone
θ	crank angle [° degrees]
δ	forced flow boundary layer [ft]
λ	electromagnetic wavelength [cm or μm]
μ	dynamic viscosity [lbm/ft-sec]
ρ	density [lbm/ft^3]
ν_k	kinematic viscosity (momentum diffusivity) = μ/ρ [ft^2/sec]
α	thermal diffusivity = $K/C_p\rho$ [ft^2/sec]
γ	ratio of specific heats = C_p/C_v

τ_w	apparent shear stress acting on the fluid at the wall [lbf/ft^2]
ε	emissivity coefficient; grey body
ε_a	apparent flame emissivity coefficient; grey body
ε_f	flame emissivity coefficient; grey body
ε_g	gas emissivity coefficient; grey body
ε_o	emissivity coefficient of infinitely thick radiating flame; grey body
ε_w	wall emissivity coefficient; grey body
τ	transmittance
α	absorptance
α_λ	monochromatic absorptance
ρ	reflectance
ρ_w	wall reflectance
σ_o	Stefan-Boltzmann constant = 1.713×10^{-9} BTU/hr-ft^2-°R^4
Δ	incremental change or difference
Δ heat	specific heat release per cycle [BTU/lbm-charge]
η	heat transfer loss/heat release per cycle
Ψ	nominal Q_R/Q_T per cycle in conventional four stroke, high r_c, direct injection CI engines

Subscripts

cp	combustion products
FC	forced convection heat transfer
NCE	New Cycle Engine
R	radiation heat transfer
T	total heat transfer
W	Woschni test engine
θ	crank angle degrees

Superscripts

$-$	mean value
$*$	corrected value

Abbreviations

BDC	bottom-dead-center
TDC	top-dead-center
BTDC	before TDC
C/H	carbon/hydrogen mass ratio
CI	compression ignition
SI	spark ignition
TI	temperature ignition

LIST OF FIGURES

List of Figures (Cont)

LIST OF TABLES

CHAPTER ONE

INTRODUCTION

1. SCOPE

Conventional compression ignition (CI) reciprocating engines have found significant application in commercial, industrial, and in land and marine transportation systems. Recent emphasis on fuel costs and availability, in conjunction with improved materials engineering, has prompted consideration of design alternatives which offer increased thermal efficiency and reduction in operating costs. A New Cycle Engine design has been proposed by Carmichael [1] in which the functions of a conventional four stroke reciprocating cylinder are divided between a compression cylinder for charge induction and compression, an expansion cylinder for charge combustion-expansion and exhaust, interconnected by a static regenerative heat exchanger.

The attractiveness of such an engine is possible because improved fabrication techniques presently allow construction of strong, thermal resistant, extremely thin-walled ceramic matrices possessing high heat transfer properties. A cyclic interchange of compressed charge into and expired exhaust gas out of the expansion cylinder via the regenerator establishes an effective medium for heat transfer and allows use of exhaust heat otherwise lost to the system. The temperature of charge air heated by adiabatic compression is boosted from the regenerator heat exchange, a direct

consequence of which is significant reduction in cylinder compression ratio, r_c, required to achieve optimum efficiency. A computer-generated thermodynamic model of this engine in preliminary design indicates that improved thermal efficiency may be achieved. An important element in the cycle analysis is accurate estimation of heat transferred from the gas medium in the expansion cylinder to its enclosing surface area, and ultimately to the coolant. The magnitude of this heat transfer reduces both heat availability to the regenerator and the thermal efficiency.

The purpose of this thesis is as follows:

1. To evaluate the applicability of existing heat transfer correlations developed to predict total mean instantaneous heat transfer coefficient, $\bar{h}_e$, in four stroke direct injection, quiescent, CI engines for prediction of total heat transfer in the New Cycle Engine expansion cylinder.
2. To evaluate and compare the magnitude of the reduction ratio in both the forced convective and the radiant heat transfer from the high peak combustion pressure conditions inherent in high r_c, CI engines to low peak combustion pressure conditions inherent in the low r_c, New Cycle Engine design.

3. To use the reduction ratios to correct existing heat transfer correlations, if applicable, and establish a correction allowing better prediction of heat transfer loss in the New Cycle Engine expansion cylinder.

2. NEW CYCLE ENGINE DESIGN BACKGROUND

A vertical cross-section of the New Cycle Engine design is provided in Figure 1-1. For simplicity, each cylinder is considered of simple geometry, with straight forward walls and flat cylinder head/piston crown configuration; bore diameter, B, equals stroke length, L. Gas velocities are boosted by piston speed, induction suction, charge impulse exiting the regenerator port, and combustion turbulence only; quiescent flow should predominate with no deliberate design feature incorporated to accelerate any rotational velocity incurred by off-set regenerator port impulse. The cylinder crank shafts will be mechanically linked to enable the compression piston to cycle at twice the speed of the expansion piston, alternating between an induction-compression and a free motoring stroke. Proper crank angle phase shift will exist to sequence the compression piston motion at the start of expansion piston down-stroke to optimize charge transfer.

Correct value timing is imperative and is sequenced through one charge cycle as follows:

1. Compression cylinder induction stroke: induction inlet valve 1 opens; regenerator transfer valve 2 is closed.
2. Compression cylinder compression stroke: valve 1 closes; valve 2 remains closed.
3. Expansion cylinder combustion-expansion stroke: regenerator exhaust value 3 closes; valve 2 opens inducing compressed charge impulse through the regenerator as the expansion piston starts the down-stroke; valve 2 then closes.
4. Expansion cylinder exhaust stroke: valve 3 opens, regenerating heat exchange capacity during exhaust gas expiration. Valve 2 remains closed; valve 1 is cycling to support the next charge cycle as expansion piston reaches top-dead-center (TDC).

A vertical cross-section schematic of the expansion cylinder and piston linkage showing principle dimensions is provided in Figure 1-2. A derivation of geometric relationships required to calculate instantaneous expansion cylinder heat transfer surface area, A_{HT}, volume, V, and piston speed, Sp, is enclosed as Appendix B. Instantaneous

expansion cylinder pressure, P, mean gas temperature, $\bar{T}g$, and volume, V, at 5° crank angle increments from the computer-generated thermodynamic model is inclosed as Appendix A, Table A-1 [1]; associated P-V and $\bar{T}g$-V diagrams for the entire cycle are illustrated in Figures 1-3 and 1-4 respectively. Other principle design and operating parameters for the expansion cylinder required to support the heat transfer calculations are listed in Appendix A. Appendices A and B provide the data point basis for the heat transfer calculations. A consideration of piston ring land area, cylinder sleeve clearances, and clearance volume, Vc, at TDC is neglected. All the area and volumetric calculations are based on simple cylinder geometry. Within the accuracy of reciprocating engine heat transfer correlations in general, errors associated with these assumptions are considered to be insignificant.

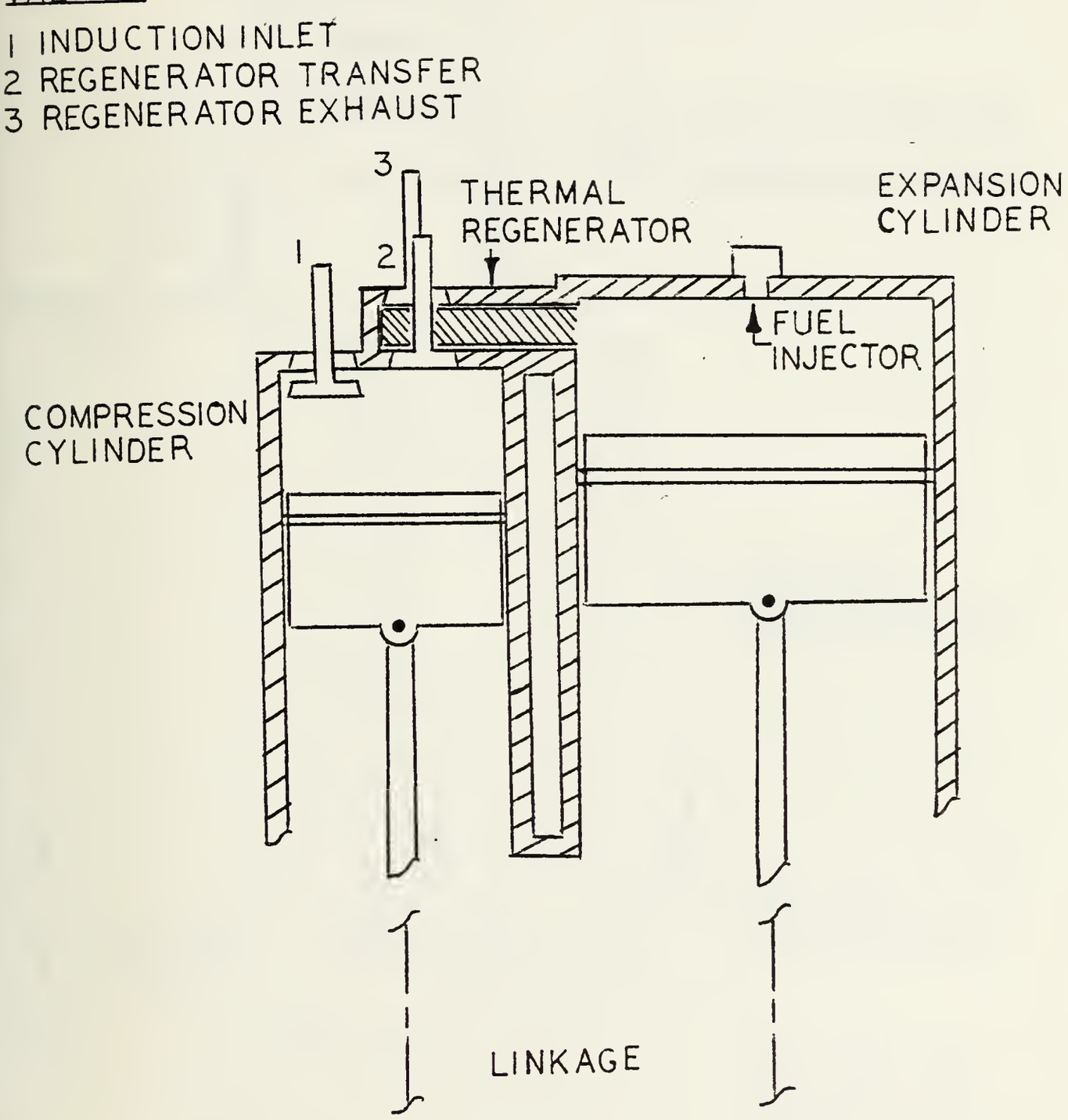

FIGURE 1-1: New Cycle Engine vertical cross-section [1]

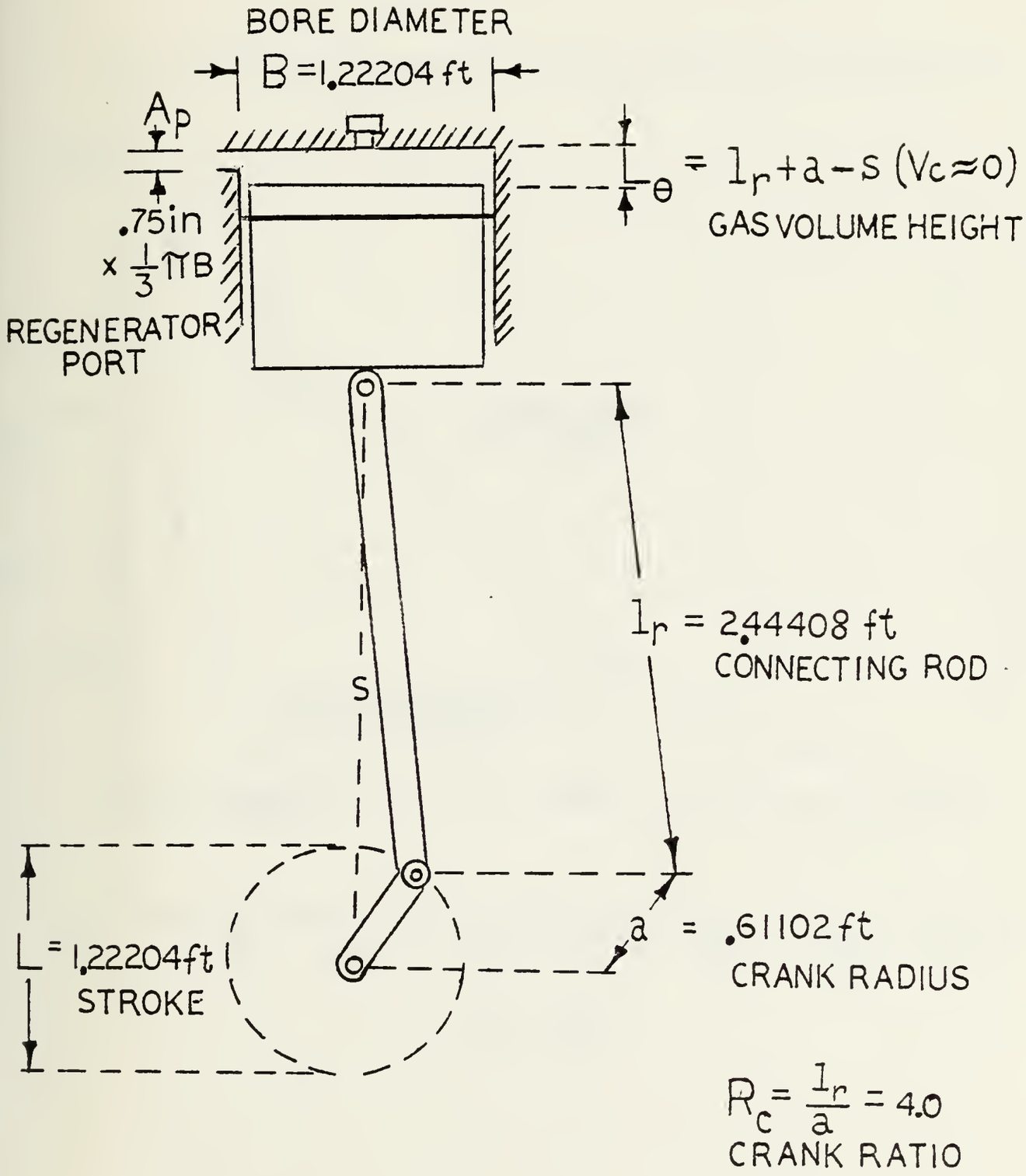

FIGURE 1-2: New Cycle Engine expansion cylinder and piston linkage dimensions [1]

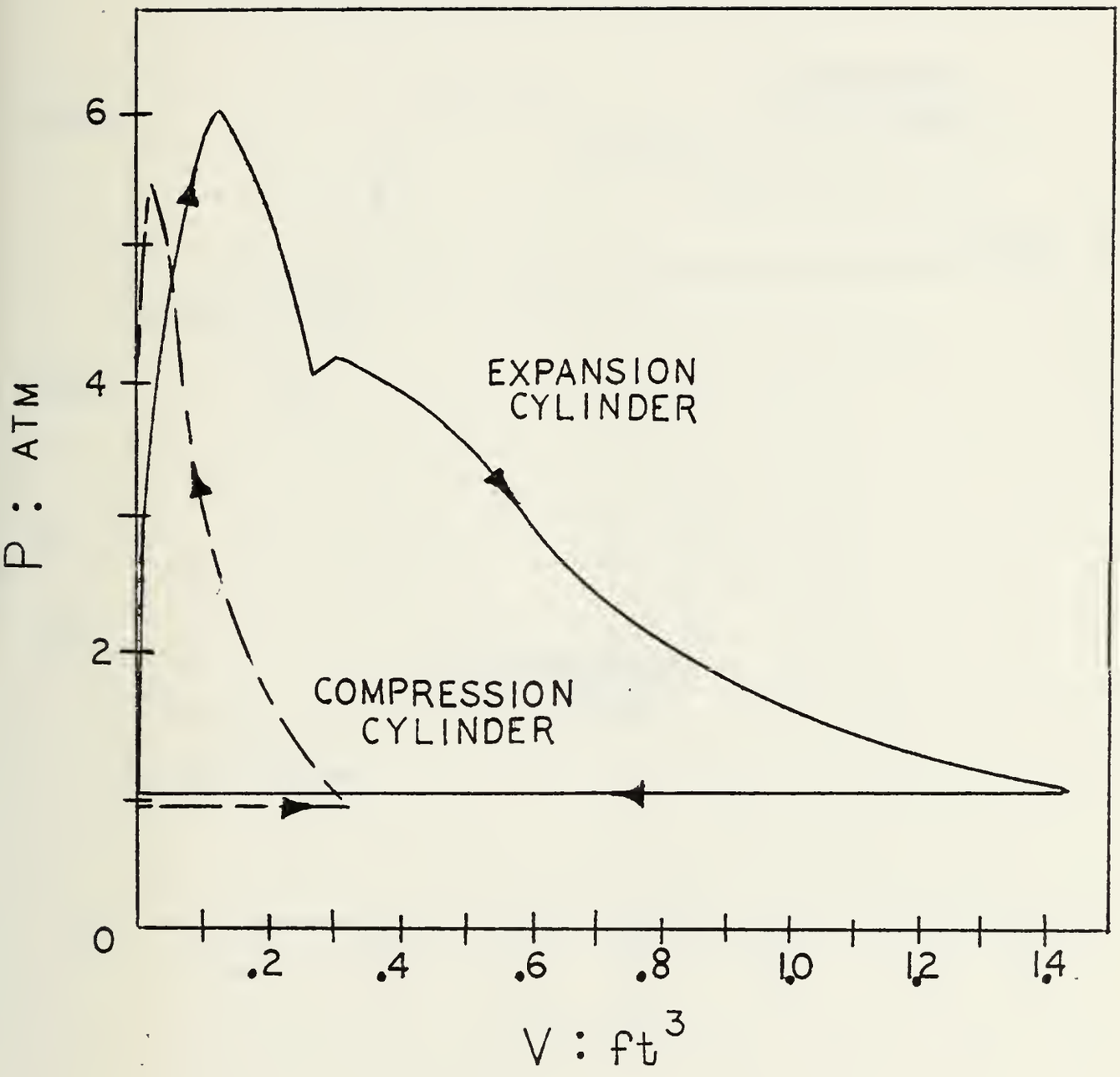

FIGURE 1-3: New Cycle Engine firing cycle P-V diagram; natural aspiration [1]

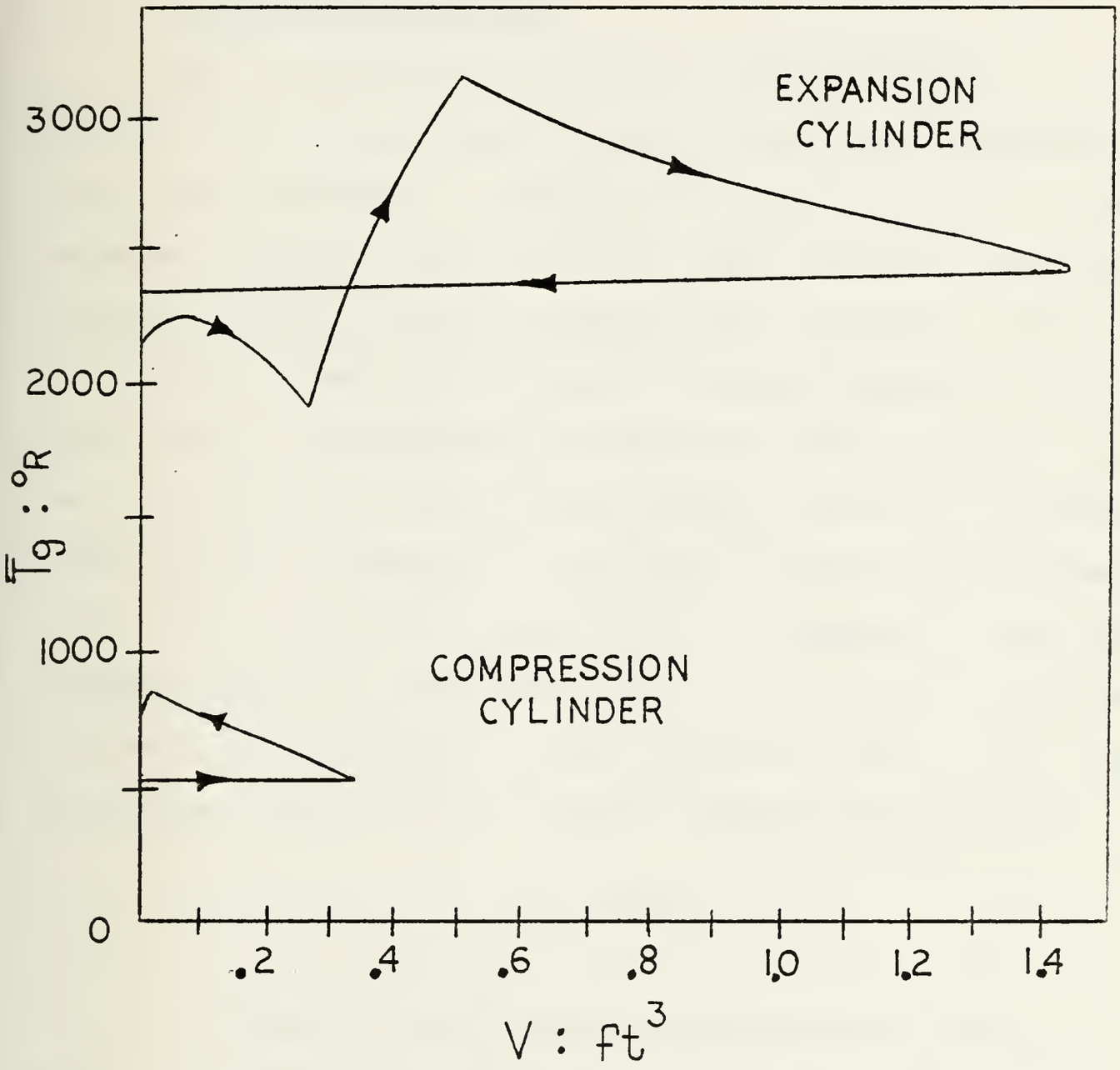

FIGURE 1-4: New Cycle Engine firing cycle $\bar{T}_g$-V diagram; natural aspiration [1]

CHAPTER TWO

FORCED CONVECTION HEAT TRANSFER IN THE NEW CYCLE ENGINE EXPANSION CYLINDER

1. THEORETICAL BACKGROUND

When a temperature difference exists between a solid surface and a moving fluid, thermal energy is transferred by the joint process of conduction and convection. Shear stresses acting on the fluid will slow the fluid immediately adjacent to the surface, forming a thin boundary layer of thickness δ. The heat transferred between the bulk fluid and the body is transported by conduction in the boundary layer as a function of fluid movement source (natural or forced), flow character (laminar or turbulent), physical properties of the fluid, and body geometry and roughness. The heat transfer rate, $\dot{Q}$, by conduction in any direction x at any instant is determined using Fourier's Law by a heat conduction coefficient, K, and the temperature gradient:

$$\dot{Q} = -KA\frac{\partial T}{\partial x} \qquad (1)$$

In laminar flow, fluid particles flowing parallel to the body surface conduct heat in a normal direction. At a certain transition velocity, turbulence is created where particles have a velocity component normal to the bulk stream direction; the intense mixing of individual layers promotes rapid transportation of heat to/from the surface. Even in turbulent flow, however, a thin boundary layer exists due to

fluid viscosity across which laminar flow and heat transfer characteristics are maintained. In turbulent systems, the heat transferred between a body surface and moving fluid remains limited by boundary layer thickness, δ, and fluid thermal conductivity, K.

An ideal linear velocity and temperature gradient across the boundary layer between a gas medium and a body surface allows approximation of the temperature gradient as $(Tg-Tw)/\delta$; substitution into equation (1) yields the Newtonian expression for steady flow conditions:

$$\dot{Q} = -KA\frac{\partial T}{\partial x}$$

$$= -KA\left[\frac{Tg-Tw}{\delta}\right]$$

$$= -\frac{K}{\delta}(Tg-Tw)$$

where letting $h \approx -\frac{K}{\delta}$:

$$\dot{Q} = hA(Tg-Tw) \qquad (2)$$

For real boundary layers of varying velocity and temperature gradients, h may be determined in some cases by integration of the differential equations describing the heat transfer process. For more general and practical applications, however, laws of similarity may be used to predict the value of h. According to the laws of similarity, it is sufficient to determine the characteristic relations between independent dimensionless groups obtained, recognizing that any such relations will apply to all similar heat transfer processes.

From the Buckingham pi theorem which allows reduction of initial variables to minimum dimensionless groups, the following dimensionless numbers are used to describe forced convection heat transfer in a fluid medium to a solid body:

1. Nusselt #, $Nu = hl_c/K$ (3)

2. Reynolds #, $Re = Ul_c/\nu_k$ (4)

3. Prandtl #, $Pr = \nu_k/\alpha = \mu C_p/K$ (5)

where: $\nu_k = \mu/\rho$ = momentum diffusivity (kinematic viscosity) (6)

$\alpha = K/C_p\rho$ = thermal diffusivity (7)

μ = dynamic viscosity

ρ = density

C_p = specific heat at constant pressure

l_c = Re characteristic length

and in general form:

Nu = function of Re, $Pr = f(Re,Pr)$ (8)

In fully developed turbulent flow systems, analysis of heat transfer processes is enhanced by a simple analogy between heat and momentum transfer which allows prediction of h from knowledge of shear stress (friction) acting on the fluid adjacent to the wall. Known as the Reynolds-Colburn Analogy, it is described by Rohsenow in the following manner [2,p.185]:

> "the heat transferred to a surface divided by the maximum amount which could be transferred in bringing the fluid to the temperature of the surface equals the momentum transferred in passing over a surface divided by the maximum amount of momentum which can be transferred in stopping the fluid relative to the surface."

This analogy, exactly true in parallel flow when Pr = 1 and reasonably accurate at Pr values not very high or very low,

may be used in either constant heat flux or wall temperature conditions and may be expressed mathematically as:

$$j \text{ Colburn factor} = StPr^{2/3} = C_f/2 \qquad (9)$$

where: Stanton #, $St = h/\rho C_p U$ (10)

$C_f = \tau_w/(\rho U^2/2)$ = friction coefficient (11)

τ_w = apparent shear stress acting on the fluid at the wall

Significant flow experimentation has determined that for low turbulent flow conditions over a smooth plate at a distance x from the leading edge:

$$C_{f_{flat\ plate}} = .0592\ Re_x^{-.2} \qquad (12)$$

Similarly, for turbulent flow conditions in a cylindrical pipe of diameter D:

$$C_{f_{pipe\ flow}} = .046\ Re_D^{-.2} \qquad (13)$$

Substitution of these relations into equation (9) allows for the determination of h:

$\bar{h}_l$, flat plate of length l:

$$StPr^{2/3} = C_f/2$$

$$\frac{h_x}{\rho C_p U} Pr^{2/3} = .0592\ (Re^{-.2})/2$$

$$h_x = .0296\ \rho C_p U (Re_x)^{-.2}\ Pr^{-2/3}$$

$$= .0296\ \rho C_p U (Re_x)^{-.2}\ Pr^{-2/3}\ \frac{x}{K}\ \frac{K}{x}$$

substituting for density, the equation (6) identity, $\rho = \mu/\nu_k$:

$$h_x = .0296 \frac{K}{x} \frac{Ux}{\nu_k} \frac{\mu C_p}{K} (Re_x)^{-.2} Pr^{-2/3}$$

recognizing equations (4) and (5) identities $Re_x = \frac{Ux}{\nu_k}$ and

$Pr = \mu C_p/K$:

$$h_x = .0296 \frac{K}{x} Re_x^{.8} Pr^{1/3}$$

integrating over length 1 to determine mean $\bar{h}_1$:

$$\bar{h}_1 = \frac{1}{1} \int_0^1 .0296 \frac{K}{x} (U_x/\nu_k)^{.8} Pr^{1/3} \, dx$$

$$= .0296 \frac{K}{1} (U/\nu_k)^{.8} Pr^{1/3} \int_0^1 x^{-.2} \, dx$$

$$= \frac{.0296}{0.8} \frac{K}{1} (U/\nu_k)^{.8} Pr^{1/3} \left[x^{.8}\right]_0^1$$

$$\bar{h}_1 = .037 \frac{K}{1} (Re_1)^{.8} Pr^{1/3} \qquad (14)$$

A similar substitution of equation (13) for turbulent flow in a cylindrical pipe yields:

$\bar{h}_D$, pipe flow of diameter D:

$$\bar{h}_D = .023 \frac{K}{D} (Re_D)^{.8} Pr^{1/3} \qquad (15)$$

These particular relations form the basis of many heat transfer correlations commonly used, rigorously applicable in fully developed, steady turbulent flow within established Re and Pr limits where temperature difference, ΔT, across the boundary layer is not extreme.

2. MODELING CONVECTIVE HEAT TRANSFER IN RECIPROCATING ENGINES

In reciprocating engines, the significant process by which termal energy is lost is by forced convective heat transfer from the gas medium across cylinder inner surface boundaries. Large variations in the magnitude and direction of convective heat transfer exist from engine to engine and point to point within an individual engine. The conditions influencing heat transfer are so complex and locally different through an engine cycle that rigorous mathematical interpretation is invalid. Radical variations in instantaneous flow patterns allow gas velocities to be only vaguely characterized. Non-uniformity of physical properties in the gas medium and surface materials exists. The combustion process is particularly difficult to model and further complicated by compression ignition. Two of the most serious obstacles question the fundamental assumption of fully developed, steady turbulent flow and the concept of a finite, instantaneous value of h.

In operating engines, the entire cycle is completed within milliseconds, making accurate measurement of local instantaneous heat flux, q, in itself quite difficult. Turbulent intensity in four stroke, CI engine cylinders is produced by the suction velocity of the induction stroke, the intensity being roughly proportional to it. To optimize fuel-air micro-mixing, off-set induction ports may be incorporated to create swirling gas motion. In the compression stroke within a simple geometry cylinder,

induction turbulence is suppressed. For swirl enhanced cylinders with combustion chambers cut into the piston crown, conservation of angular momentum in the cup created by viscous drag accelerates swirl to significant angular velocities as the piston reaches TDC. Radial "squish" velocities are created near TDC and combine with swirl to produce a complicated toroidal motion. In the expansion stroke, rapid deacceleration of rotational velocities in direct injection cylinders are superimposed by ill-defined, small combustion induced velocities as hot combustion product gases expand; in indirect injection cylinders, prechambers deliberately channel and exaggerate the charge velocities to blow out of energy cells at levels up to 500m/sec [3]. In the exhaust stroke, the combustion products are pushed out by the piston. The accumulation of these factors indicate that turbulent boundary layers are not steady, but are periodically created and destroyed in a manner beyond our ability to model. In addition, because of the thermal capacity of the gases, there is a thermodynamic phase lag markedly apparent in reciprocating engines; ΔT and q do not pass through zero at the same instant indicating values of $h = \pm\infty$ and highly fluctuating values immediately about it.

Recognizing these obstacles, investigators have concluded that within obtainable accuracy it is still best to model heat transfer as a quasi-steady process and to correlate cyclic observations in terms of conventional Nu, Re, Pr numbers. Values of the various constants and

exponents are determined in individual engine tests; a wealth of experimental data provides guidance for constant(s) selection for operating engines or design studies of similar construction. Hohenberg states [4, pg. 2788]:

> "It would be erroneous to look for a formulation which includes all possible influences on the heat transfer. This would only render the calculation more complicated rather than more accurate. The aim...must be to find out and mathematically describe the really essential factors influencing heat transfer in the engine."

If the time for change in bulk stream conditions to diffuse through a boundary layer is small relative to other significant times in the engine cycle, then boundary layers may be considered quasi-steady and at any instant be that associated with existing conditions. Le Feuvre et al [5] approximating diffusing time as δ^2/ν_k and modeling gas motion in solid body rotation, successfully performed such calculations in a direct injection, swirl enhanced, CI engine operating at high RPM (2000 RPM). As for the existence of phase lag, Annand [6] states that the actual quantity of heat transferred during this period is minute; the error arising from the use of a finite h at each instant of the piston stroke is negligible.

The majority of the heat transferred within a reciprocating CI engine is due to turbulent forced convection. On the basis of experimental data and theoretical considerations, this relationship is expressed by the formula:

$$Nu = \text{constant}(R_e)^n \, Pr^i \qquad (16)$$

Recognizing that Pr ≈ 0.7 for common gas mediums due to predominance of O_2 and N_2, substitution of the ideal gas law identity, $\rho = P/R\bar{T}g$, into an expanded equation (16) yields:

$$h = \text{constant } K\mu^{-n}P^{n}U^{n}\bar{T}g^{-n}l_c^{n-1} \qquad (17)$$

Assuming that actual gas velocities will be at least approximately proportional to mean piston speed, a function of $\bar{S}p$ is used with the multiplicity constant determined by engine design. $\bar{T}g$ is used vice the average, $(\bar{T}g + \bar{T}w)/2$, as the calculation of $\bar{T}g$ from measured instantaneous pressure and gas law application already represents an average for the cylinder contents. A consideration of gas disassociation is neglected, as any attempt to quantify it would be eclipsed by the previous assumption of uniform properties. During the combustion process, gas product composition is assumed to equal the burned composition. Tables and Figures of thermal properties (μ, C_p, Pr, γ) for individual gases and C_nH_{2n} lean hydrocarbon fuel combustion products are provided in Appendix C [6,7]. Cyclic local instantaneous surface temperature profiles, from which actual measurement of q is generally derived, are demonstrated by Oguri et al [8] to show transient magnitudes typically less than 50°F for sooty surfaces and less than 20°F for clean surfaces. With the exception of exhaust valve/port entries which may typically see temperatures greater than 1000°F, the temperature range exhibited by cylinder sleeve, head, and piston crowns are fairly consistent allowing assumption of a mean $\bar{T}w$.

3. WOSCHNI'S CORRELATION FOR MEAN INSTANTANEOUS HEAT TRANSFER COEFFICIENT, $\bar{h}_e$, IN CI ENGINES

A recognized industry standard for four stroke, direct injection, quiescent, CI engine heat transfer calculation is Woschni's correlation, stated in U.S. units as follows [9]:

$$\bar{h}_e = 15.480\, P^{.8}[C_1 \bar{S}p + C_2 (V\bar{T}g_c / P_c V_c)(P-Po)]^{.8} B^{-.2} \bar{T}g^{-.53} \quad (18)$$

where $\bar{h}_e$ = BTU/hr-ft^2-°R

P_c, V_c, $\bar{T}g_c$ = instantaneous values at ignition start

Po = motoring pressure

Based on suppressed swirl engine designs, the values of constants C_1 and C_2 are:

1. induction stroke $C_1 = 6.18$ $C_2 = 0$ (18a)
2. compression stroke $C_1 = 2.28$ $C_2 = 0$ (18b)
3. expansion stroke (motoring) $C_1 = 2.28$, $C_2 = 0$ (18c)
4. combustion-expansion stroke $C_1 = 2.28$, $C_2 = 5.9054 \times 10^{-3}$ ft/sec-°R (18d)
5. exhaust stroke $C_1 = 6.18$ $C_2 = 0$ (18e)

From equation (17), a n exponent of 0.8 was determined by Woschni by successively changing one parameter at a time over maximum possible range. A consensus opinion of all recent published correlations is that $0.7 \leq n \leq 0.8$, reflecting agreement with the laws of similarity. Woschni developed the motoring/firing correlation and scavenging correlation on suppressed swirl design cylinders stating [9,p.3071]:

> "The gas motion generated during the induction phase dies away with time, owing to internal friction. In the compression stroke, however, dependent upon the piston or cylinder cover shape, an additional gas motion can be induced [squish-swirl] whose intensity is also proportional to piston speed. In this particular case, the engine involved had direct injection and straight forward combustion chamber walls, so that decay due to internal friction prevailed."

A $\bar{T}g^{-.53}$ exponent is due to Woschni's assumption of air and gas product $\mu(\bar{T}g) \propto \bar{T}g^{.6}$ and $K(\bar{T}g) \propto \bar{T}g^{.75}$ at n exponent = 0.8 (see equation (17)). To approximate ill-defined velocity increase due to combustion, the difference P-Po which, unlike $\bar{T}g-\bar{T}o$, sees a rapid decay upon combustion completion, is used, multiplied by instantaneous cylinder volume, V, and related to the charge mass at beginning of combustion, $m_c = P_cV_c/R\bar{T}g_c$.

It is at this point that Woschni makes a critical simplifying assumption. Recognizing the significant effect of luminous flame radiation heat transfer in CI engines, Woschni arbitrarily accounts for combustion radiant heat transfer by affixing the value C_2 to equate actual measured $\dot{Q}$ integrated over the stroke with Q combustion determined by the correlation. Woschni states [9,p.3075]:

> "There is no doubt that such an influence occurs in the engine, and it is taken into consideration in lumped form in the combustion term as defined here, but it seems impossible to the author to separate it from the convective term. The only question that remains to be considered, therefore, is the error made regard to the tendency...for the radiation."

In essence, for application to the New Cycle Engine expansion cylinder operating at significantly lower peak pressure conditions, laws of similarity allow significant extrapolation of Woschni's correlation for forced convection heat transfer only. The correlation must be corrected to account for the fact that radiant heat transfer is not a function of $(P-Po)^{.8}$.

4. CALCULATION OF ORDER OF MAGNITUDE REDUCTION IN COMBUSTION FORCED CONVECTION HEAT FLUX

The representative firing cycle P-$\bar{T}g$ versus crank angle plot published by Woschni for natural aspirating operation is shown as Figure 2-1 [9]. The range of additional principle operating parameters over which the motoring/firing correlations were developed well representive the essential parameters of New Cycle Engine (NCE) expansion cylinder operation [9]:

Parameter	Woshni (W) engine	NCE Expansion Cylinder
RPM	900 max	818.3
$\bar{S}p$	9 m/s max [29.6 f/s]	33.$\bar{3}$3 ft/sec
Supercharge pressure ratio	3 max	1.0
$\bar{T}w$	nominal 500°K [900°R]	900°R
L,B	unknown	1.22204 ft

Bore and stroke dimensions were not provided, however from known maximum data point values $\bar{S}p$ = 9 m/sec and N_{RPM} = 900, the approximate stroke length L may be determined:

$$L \approx \frac{60}{2N_{RPM}} \bar{S}p \approx \frac{(60)(9)}{(2)(900)} \approx 0.3 \text{ m } [0.98 \text{ ft}] \text{ approx.}$$

For conventional CI engine geometry, bore diameter B is approximately equal to L; therefore for effective comparison of $\bar{h}_e$ proportional to $B^{-.2}$ in forced convection heat transfer, consideration of bore diameters of similar magnitude dimensions may be neglected. The significant difference between combustion-expansion stroke profiles are:

1. An order of 15 magnitude increase in peak combustion pressure in Woschni's conventional high r_c, CI engine.
2. A reduced $\bar{T}g$ decay rate, thus increased $(\bar{T}g-\bar{T}w)$ forced convective heat transfer potential in the New Cycle Engine expansion cylinder.
3. A delayed fuel injection/ignition start in the New Cycle Engine expansion cylinder.

Assuming that the magnitude of mean instantaneous gas velocities through the expansion strokes are roughly equal, the approximate ratio of forced convective heat transfer loss in the respective engines may by obtained by determining the mean ratio of instantaneous heat flux, q, over a 90° crank angle domain from ignition start. A selection of 90° is based on:

1. Establishing a normalized basis in which to compare the order of magnitude reduction in

forced convection versus radiant heat transfer; the crank angle domain over which luminous flame radiation is significant in medium speed CI engines less than 1000 RPM is nominally 90° from combustion start [8].

2. At 90° the slope of pressure and temperature decay transients induced by combustion in both engines become small.

Setting the radiant heat transfer constant $C_2 = 0$ in equation (18d):

$$q_W/q_{NCE} \propto \bar{h}_e(\bar{T}g-\bar{T}w)_W/\bar{h}_e(\bar{T}g-\bar{T}w)_{NCE}$$

$$q_W/q_{NCE} \propto \frac{[P^{.8}\bar{S}p^{.8}/B^{.2}\bar{T}g^{.53}][\bar{T}g-\bar{T}w]_W}{[P^{.8}\bar{S}p^{.8}/B^{.2}\bar{T}g^{.53}][\bar{T}g-\bar{T}w]_{NCE}}$$

Neglecting B consideration and assuming equal magnitude gas velocities:

$$\frac{q_W}{q_{NCE}} \propto \frac{[P^{.8}/\bar{T}g^{.53}][\bar{T}g-\bar{T}w]_W}{[P^{.8}/\bar{T}g^{.53}[\bar{T}g-\bar{T}w]_{NCE}} \qquad (19)$$

where $\bar{T}w = 900°R$

Table 2-1 summarizes the calculations based on Figure 2-1 and Appendix I data at 5° increments from combustion start. The mean heat flux reduction ratio may then be determined by numerical integration using Simpson's rule:

$$\frac{\bar{q}_w}{q_{NCE_{forced\ convection}}} = \frac{1}{\Delta 90^\circ} \int_0^{90} [q_w/q_{NCE}]d\theta \quad (20)$$

$$\frac{\bar{q}_w}{q_{NCE}} = \frac{\frac{\Delta 5^\circ}{3}\left[1\frac{q_w}{q_{NCE_{0^\circ}}} + 4\frac{q_w}{q_{NCE_{5^\circ}}} + 2\frac{q_w}{q_{NCE_{10^\circ}}} + \ldots + 2\frac{q_w}{q_{NCE_{80}}} + 4\frac{q_w}{q_{NCE_{85}}} + 1\frac{q_w}{q_{NCE_{90^\circ}}}\right]}{\Delta 90^\circ}$$

$$= \frac{\Delta 5^\circ/3\ [328.67]}{90^\circ} = 6.087 \text{ approx.}$$

TABLE 2-1

Calculation of order of magnitude reduction in combustion forced convection q from Woshni's test engine to New Cycle Engine expansion cylinder operation at 5° crank angle increments

Crank angle	Woshni engine (W)				NCE Expansion Cylinder		q_W/q_{NCE}
past ignition start	P kp/cm^2	$\bar{T}g$ °K	P atm	$\bar{T}g$ °R	P atm	$\bar{T}g$ °R	equation (19)
0	40	875	38.71	1575.0	4.15	1896.6	4.46
5	60	1400	58.07	2520.0	4.25	2252.6	9.14
10	63	1525	60.97	2745.0	4.09	2571.2	9.29
15	60	1600	58.07	2880.0	3.92	2864.1	8.68
20	55	1650	53.24	2970.0	3.76	3136.0	7.94
25	47	1630	45.49	2934.0	3.26	3064.2	7.92
30	40	1600	38.71	2880.0	2.89	2998.7	7.68
35	33	1540	31.94	2772.0	2.59	2939.1	6.66
40	26	1480	25.16	2664.0	2.34	2884.8	6.2
45	22.5	1440	21.18	2592.0	2.13	2835.2	5.76
50	20	1400	19.36	2520.0	1.96	2790.0	5.65
55	17	1365	16.45	2430.0	1.81	2748.8	5.16
60	15	1330	14.52	2394.0	1.69	2711.3	4.92
65	12.5	1305	12.1	2349.0	1.58	2677.1	4.46
70	11	1280	10.65	2304.0	1.49	2646.0	4.17
75	10	1255	9.68	2259.0	1.42	2617.8	3.97
80	9	1230	8.71	2214.0	1.35	2592.3	3.75
85	8.5	1215	8.23	2187.0	1.3	2569.2	3.68
90	8	1200	7.74	2160.0	1.25	2548.4	3.59

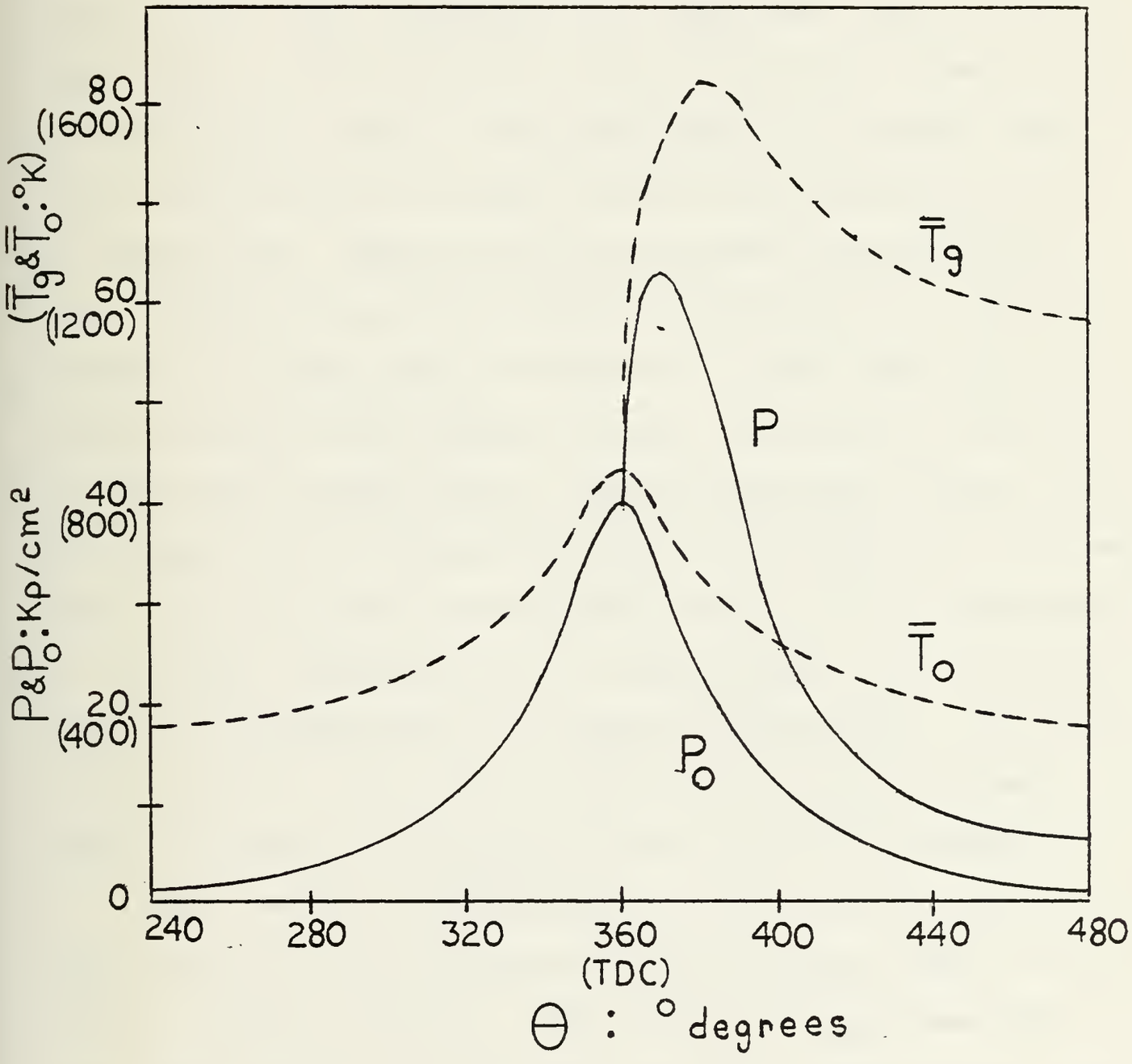

FIGURE 2-1: Woschni's test engine firing cycle; natural aspiration [9]

5. ESTIMATION OF MEAN GAS VELOCITY MAGNITUDE, $\bar{U}$

5.1 CONSTRUCTION OF CHARGE IMPULSE VELOCITY, Ui, TRANSIENT

Acceptance of the general applicability of Woschni's correlation to the New Cycle Engine expansion cylinder balances on the assumption of comparable gas velocity magnitudes. While geometric flow patterns are indeterminate in preliminary design, the magnitude of the charge impulse into the expansion cylinder leaving the regenerator port can be ascertained. Recognizing the inevitable deacceleration of this impulse in a simple geometry cylinder on the expansion stroke, a conservative estimation of the mean bulk gas velocity at the walls, $\bar{U}exp$, through the expansion stroke can be made with minimum error. Substituting $\bar{U}exp$ directly into the steady, fully developed turbulent flow equations (14) and (15) for flat plate and pipe flow should, if the magnitudes of cylinder velocities are in fact similar, be reasonably close to $\bar{h}_e$ calculated from Woschni's correlation. To reduce uncertainties, the relationships will be first compared in motoring conditions from TDC to 45°, prior to ignition start.

Dent et al [10] successfully used a similar method in approximating forced convective heat transfer loss in a four stroke, direct injection, high swirl, CI engine operating at peak TDC swirl ratios equal to 20. Predictions using Woschni's motoring correlations failed uniformly low compared to measured, spatially averaged, instantaneous heat flux. This is expected, considering the central assumption of suppressed swirl inherent in application of Woschni's

correlation. By substituting directly into the flat plate h equation (14), measured instantaneous angular gas velocity ω_r at l_c equal to bore circumference ($2\pi r$), remarkable agreement was obtained. Agreement was not as good at firing conditions due to the transient combustion processes.

From ideal gas law, at a given angle θ in the expansion stroke, charge mass, m, in the expansion cylinder:

$$m_{\theta\ lbm} = \frac{PV}{R\bar{T}g} = \frac{(2116.224\ lbf/ft^2\text{-}atm)PV}{(53.90)\bar{T}g}$$

$$= 39.262\ \frac{PV}{\bar{T}g} \qquad (21)$$

Taking 5° crank angle as the unit increment of time at 818.3 RPM; the charge mass rate, entering the expansion cylinder is:

$$\dot{m}_{\theta\ lbm/sec} \approx \frac{\Delta m(5°)}{\Delta t(5°)} = \frac{\Delta m(5°)}{\frac{1}{(N_{RPM}/60)}\frac{5}{360°}}$$

$$= \frac{\Delta m(5°)}{.0010184\ sec} \qquad (22)$$

The continuity equation for impulse flow leaving the regenerator port cross-section area, A_p, equal to 0.80 ft^2 is:

$$\dot{m}_\theta = \rho U_i A_p \qquad (23)$$

Therefore, by rearranging equation (23), impulse velocity leaving the regenerator port, U_i, can be determined:

$$Ui_{ft/sec} = \frac{\dot{m}_\theta R \bar{T}g}{PA_p} = \frac{\dot{m}_\theta (53.90)\bar{T}g}{(2116.224\ lbf/ft^2\text{-}atm)P(.080)}$$

$$= \frac{.31837\ \dot{m}_\theta\ \bar{T}g}{P} \qquad (24)$$

A summary of the calculations using instantaneous P, $\bar{T}g$, V values from Appendix A at 5° increments is provided in Table 2-2. Charge mass as a function of expansion stroke crank angle is plotted in Figure 2-2, indicating that the main impulse from the compression cylinder via the regenerator exit port completes 10° past ignition start.

At 45° combustion start $\%m_{total} = \frac{2.1905 \times 10^{-2}}{2.4537 \times 10^{-2}} = 89.3\%$

At 55° main impulse completion
$\%m_{total} = \frac{2.28894 \times 10^{-2}}{2.4537 \times 10^{-2}} = 93.3\%$

Ui as a function of expansion stroke crank angle is plotted in Figure 2-3, indicating a peak Ui equal to 519.95 ft/sec near fuel injection start (30°).

TABLE 2-2

Calculation of charge Ui leaving the regenerator port into the New Cycle Engine expansion cylinder at 5° crank angle increments

Crank Angle	m	$\Delta m_{5°}$	$\dot{m}$	Ui
θ°	lbm eq.(21)	ΔlbmE-3	lbm/sec eq.(22)	ft/sec eq.(24)
TDC	0	0	0	0
5	1.5550E-4	0.1555	0.1527	41.82
10	7.7090E-4	0.6154	0.6043	133.14
15	2.1309E-3	1.360	1.3275	236.92
20	4.5821E-3	2.451	2.4069	352.69
25	8.3113E-3	3.730	3.6618	458.13
30	1.2936E-2	4.625	4.5413	519.95
35	1.7373E-2	4.437	4.357	499.15
40	2.0491E-2	3.118	3.0614	382.68
45	2.1905E-2	1.414	1.3882	202.03
50	2.2887E-2	0.9816	0.9641	162.73
55	2.2889E-2	0.0028	0.00275	0.55
60	2.2932E-2	0.0426	0.04183	9.72
65	2.2992E-2	0.0596	0.05852	15.54
70	2.3056E-2	0.0641	0.06294	18.83
75	2.3307E-2	0.2510	0.2465	81.44
80	2.3512E-2	0.2049	0.2012	72.76
85	2.3680E-2	0.1687	0.1657	65.12
90	2.3820E-2	0.1397	0.1372	58.15
95	2.3937E-2	0.1167	0.1146	52.03
100	2.4035E-2	0.0981	0.09633	46.56
105	2.4118E-2	0.0827	0.08121	41.54
110	2.4188E-2	0.0702	0.06893	37.12
115	2.4247E-2	0.0596	0.05852	33.0
120	2.4298E-2	0.0511	0.05018	29.84
125	2.4342E-2	0.0436	0.04281	26.13
130	2.4379E-2	0.0372	0.03653	23.04
135	2.4411E-2	0.0320	0.03142	20.41
140	2.4438E-2	0.0270	0.02651	17.67
145	2.4462E-2	0.0239	0.02347	15.99
150	2.4480E-2	0.0183	0.01797	12.48
155	2.4496E-2	0.0158	0.01552	10.94
160	2.4509E-2	0.0130	0.01276	9.12
165	2.4519E-2	0.0101	0.00992	7.15
170	2.4527E-2	0.0074	0.00727	5.28
175	2.4532E-2	0.0051	0.00501	3.65
BDC	2.4537E-2	0.0052	0.00511	3.70

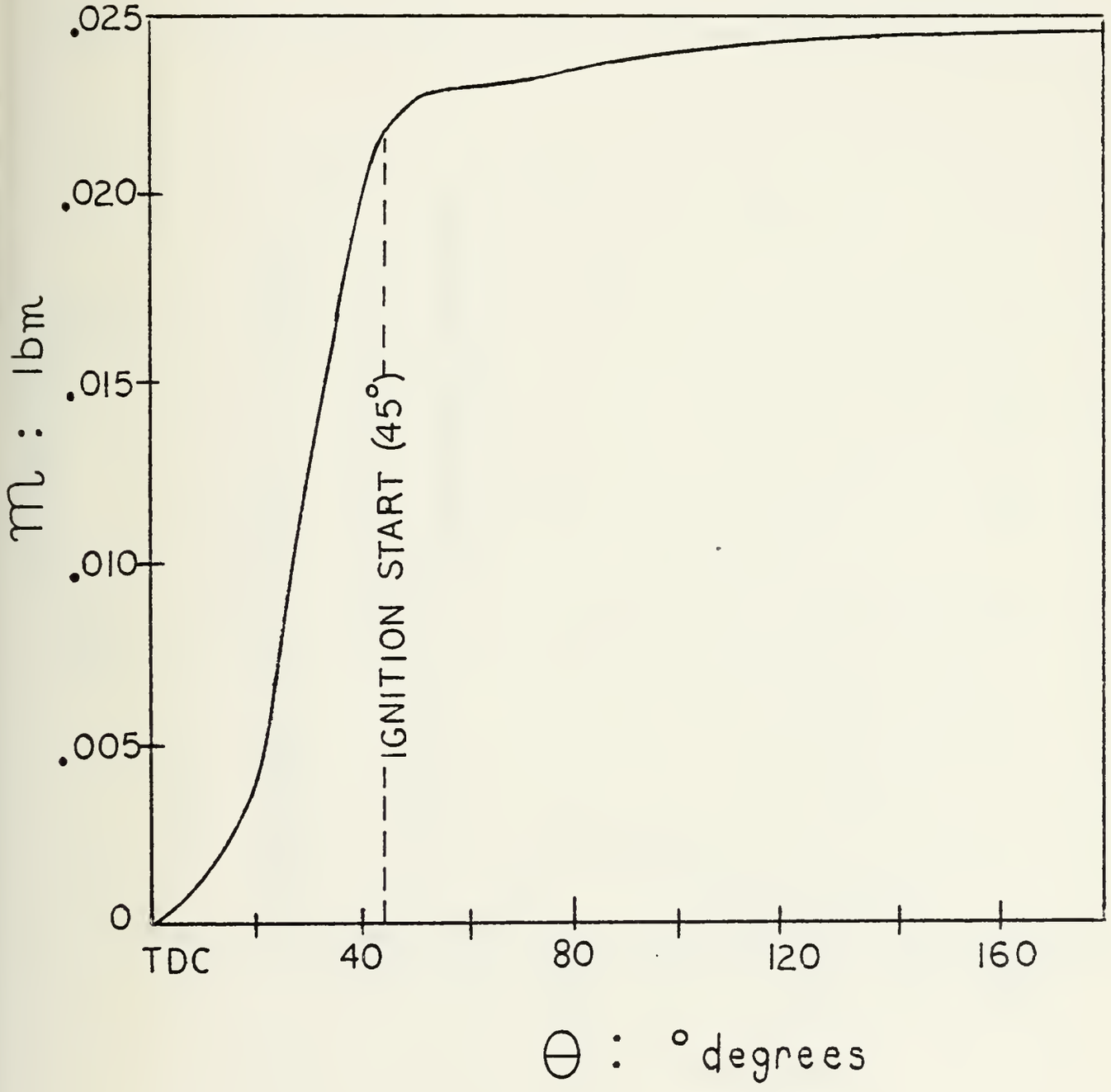

FIGURE 2-2: Expansion cylinder mass charge, m, versus expansion stroke crank angle

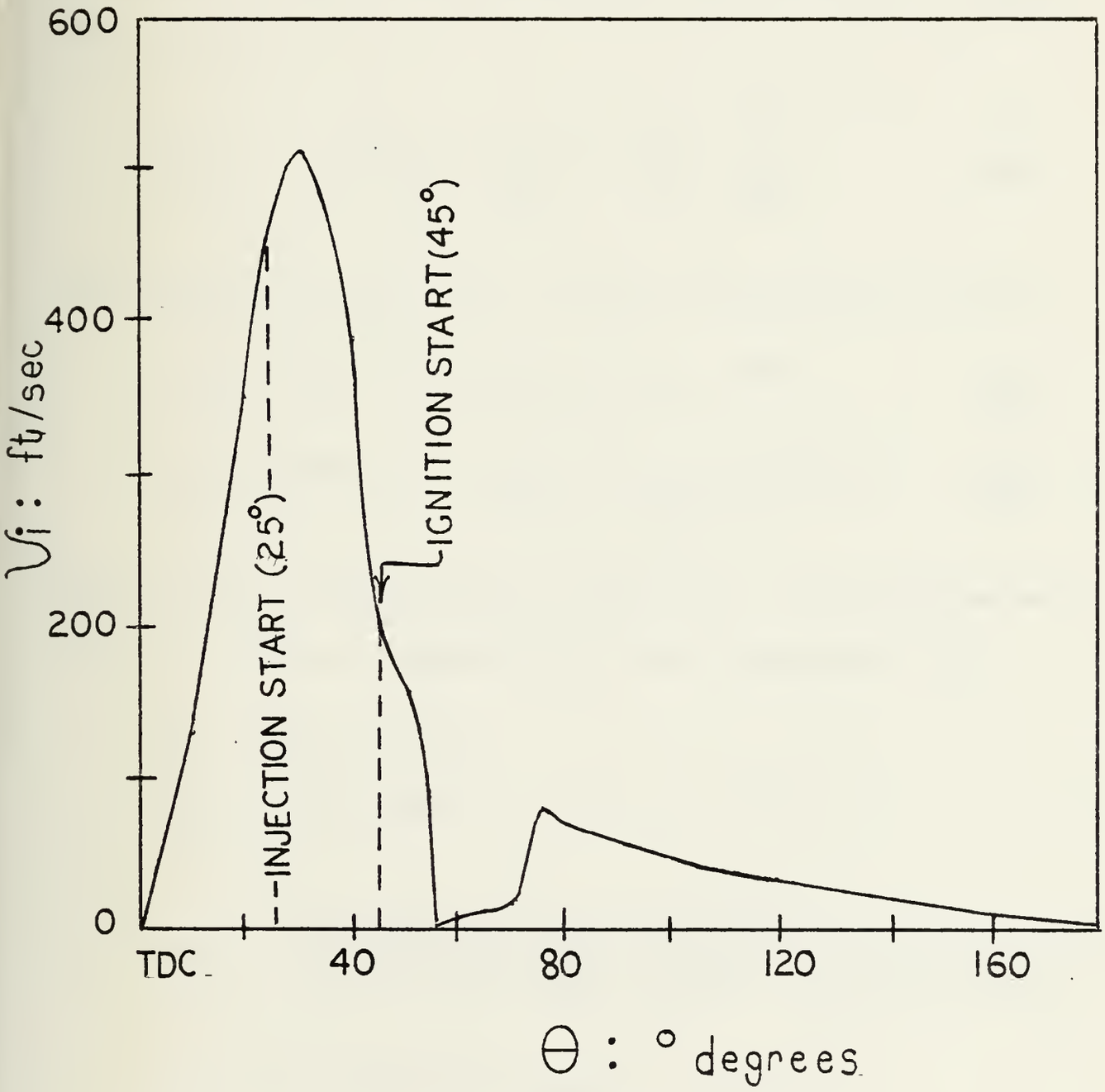

FIGURE 2-3: Expansion cylinder charge V_i versus expansion stroke crank angle

5.2 VERIFICATION OF TURBULENT FLOW

To verify turbulent flow conditions leaving the regenerator port, calculated Re at 30° using l_c equal to the regenerator port cross-section minor dimension (depth) of 0.75 inch is:

$$Re_{30°} = \frac{Uil_c}{\nu_k} = \frac{Uil_c}{\mu/\rho} = \frac{\rho Uil_c}{\mu} \cdot \frac{P}{R\bar{T}g} \qquad (25)$$

From Appendix C, Table C-1, $\mu(\bar{T}g)$ and $C_p(\bar{T})$ for air is:

$$\mu \text{ lbm/ft-sec} = 2.163 \times 10^{-7} (\bar{T}g)^{.645} \qquad (26) \quad (C1)$$

$$C_p \text{ BTU/lbm-hr} = 0.224 + 0.262 \times 10^{-4} \bar{T}g \qquad (27) \quad (C2)$$

Substituting instantaneous values of P, $\bar{T}g$ from Appendix A and $\mu(\bar{T}g)$ identity equation (26) into equation (25):

$$P_{30°} = 6.10171 \text{ atm}$$

$$\bar{T}g_{30°} = 2194.29°R$$

$$Re_{30°} = \frac{(519.95)(0.75/12)(2116.224 \text{ lbf/ft}^2\text{-atm})(6.10171)}{(2.163 \times 10^{-7})(2194.29)^{.645} \quad (53.90)(2194.29)}$$

$$= 1.1476 \times 10^5 \text{ turbulent}$$

5.3 ESTIMATION OF EXPANSION STROKE, $\bar{U}exp$

The calculation of the mean impulse velocity, $\bar{U}i$, for the purpose of $\bar{U}exp$ approximation, is correctly restricted to the main impulse domain TDC to 55° only, neglecting residual 10% charge mass regenerator bleed. Combustion induced perturbations during crank angles 45°-55° may be neglected. Ui may then be calculated using numerical integration by trapezoidal rule and is equal to:

$$\bar{U}i_{\substack{ft/sec \\ TDC-55°}} = \frac{1}{\Delta 55°}\int_{TDC}^{55°} Ui \, d\theta \qquad (28)$$

$$= \frac{(\Delta 5°/2)[\, Ui_{TDC} + 2Ui_{5°} + 2Ui_{10°} \ldots + 2Ui_{50°} + Ui_{55°}\,]}{\Delta 55°}$$

$$= \frac{(\Delta 5°/2)[5979.03]}{\Delta 55°} = 271.77 \text{ ft/sec}$$

A reasonable assumption must be made as to the expected value of $\bar{U}exp$ over the entire stroke. The principle factors causing charge velocity deacceleration include cross-section area expansion exiting the regenerator port, internal friction, cylinder volumetric expansion, and angular momentum deacceleration of any existing rotating flow patterns. References [5, 10, 11, 12, 13] unanimously agree that in swirl enhanced engines, peak instantaneous swirl at TDC is much greater than the mean swirl valves over the stroke. Le Feuvre et al [5] calculated for a 4.5 inch bore direct injection, CI engine operating at 2000 RPM, that 10% velocity

decrease occurred each stroke due to viscous dissipation alone. A conservative estimate of $\bar{U}exp = (\bar{U}i_{TDC-55°})/2$ is therefore assumed; selection of this value should reduce any error in either direction. It is noted that $\bar{U}i_{TDC-BDC}$ from Table 2-2 in firing conditions equals 102.9 ft/sec. Combustion induced velocities due to charge gas expansion in spark ignition (SI) engines have been calculated by Annand [3] to be on the order of 33 ft/sec, with expected velocities in CI engines less due to diffusion flame configuration. Thus, let $\bar{U}exp = (\bar{U}i_{TDC-55°})/2 = 135.9$ ft/sec.

6. COMPARISON OF $\bar{h}_e$ CALCULATED FROM WOSHNI'S CORRELATION AND THEORETICAL MODELS

6.1 EXPANSION STROKE; MOTORING CONDITION

Using the above first approximation of $\bar{U}exp$, estimates of $\bar{h}_e$ from theoretical equations (14) and (15) for steady, fully developed flow may be reached. Expanding pipe flow equation (15) at $l_c = B$ and $U = \bar{U}exp$ yields:

$$\bar{h}_D = .023(K/B)Re_D^{.8}Pr^{1/3} = .023(K/B)[\bar{U}expB/\nu_k]^{.8}Pr^{1/3}$$

Substituting the identities $\nu_k = \mu/\rho$, $K = C_p\mu/Pr$, and $\rho = P/R\bar{T}g$:

$$\bar{h}_D = .023C_p\mu[P\bar{U}exp/\mu R\bar{T}g]^{.8}B^{-.2}Pr^{-2/3}$$

Substituting the $C_p(\bar{T})$ and $\mu(\bar{T}g)$ identities from equations (27) and (28) and appropriate conversions:

$$h_D = .023[.224+.262x10^{-4}\bar{T}g][2.163x10^{-7}(\bar{T}g)^{.645}(3600sec/hr)]*$$
$$[(2116.224\ lbf/ft^2\text{-}atm\ P\ \bar{U}exp)/(2.163x10^{-7}\bar{T}g^{.645}R\bar{T}g)]^{.8}*$$
$$B^{-.2}Pr^{-2/3}$$

which simplifies at known R, $\bar{U}exp$, Pr values to:

$$\bar{h}_{D\ BTU/hr\text{-}ft^2\text{-}^\circ R} = 9.194[2.24+2.62x10^{-4}\bar{T}g]\frac{(135.9\ P)^{.8}}{B^{.2}\ \bar{T}g^{.671}} \quad (29)$$

An identical expansion of the flat plate equation (14) at $l_c = \pi B$, expansion cylinder circumference, yields:

$$\bar{h}_{1\ BTU/hr\text{-}ft^2\text{-}^\circ R} = 11.674[2.24+2.62x10^{-4}\bar{T}g]\frac{(135.9\ P)^{.18}}{B^{.2}\ \bar{T}g^{.671}} \quad (30)$$

A summary of $\bar{h}$ calculations for the charge induction monitoring angles, TDC-45°, comparing equations (29) and (30) to Woshni's motoring correlation equation (18c), is provided in Table 2-3. The agreement is quite good, even with acceptance of reasonable error in $\bar{U}exp$ approximation.

TABLE 2-3

Comparison of $\bar{h}_e$ calculated by Woshni's correlation and theoretical models during charge induction into the New Cycle Engine expansion cylinder

Crank Angle θ°	$\bar{h}_e$ eq.(18c)	$\bar{h}_D$ eq.(29)	$\bar{h}_1$ eq.(30)
5	16.994	15.221	19.477
10	20.191	18.143	23.215
15	24.006	21.593	27.631
20	28.209	25.396	32.496
25	32.029	28.839	36.902
30	34.236	30.793	39.403
35	33.888	30.414	38.918
40	31.168	27.897	35.697
45	27.164	24.251	31.037

h in BTU/hr-ft^2-°R

6.2 EXHAUST STROKE

Attempts to directly estimate the mean bulk gas velocity at the walls during the exhaust stroke, $\bar{U}exh$, in light of preliminary design restrictions and post-combustion ambiguities, are not valid.

An indirect method allowing $\bar{h}$ calculation is to correct equation (29) by a factor equivalent to the scavenging/motoring $\bar{U}exh$ correction observed by Woschni for suppressed swirl geometry, direct injection, CI engine cylinders. From equations 18a and 18c:

$$\bar{U}exh \text{ correction factor} = (6.18\ \bar{S}p/2.28\ \bar{S}p)^{.8} = 2.22$$

When the regenerator exit valve 3 opens, the significant flow pattern will be parallel to the bore axis, up the sleeve, and through the regenerator port; flow direction is therefore analogous to pipe flow. From Appendix C, the identities $\mu(\bar{T}g)$, $C_p(\bar{T}g)$, $Pr(\gamma)$, and $\gamma(\bar{T}g)$ for lean C_nH_{2n} hydrocarbon fuel combustion products at P = 1 atm, Φ = 0.75 may be calculated:

$$\mu \text{ lbm/ft-sec} = \frac{1.47\times10^{-7}(\bar{T}g)^{.7}}{1 + .027\Phi} = \frac{1.47\times10^{-7}(\bar{T}g)^{.7}}{1 + .027(.75)}$$

$$= 1.441\times10^{-7}(\bar{T}g)^{.7} \qquad (31)\ (C3)$$

$$C_p \text{ BTU/lbm-°R} = 0.247 + 0.243\times10^{-4}\ \bar{T}g \qquad (32)\ (C5)$$

$$Pr(\gamma) = 0.05 + 4.2(\gamma-1) - 6.7(\gamma-1)^2 \qquad (33)\ (C4)$$

$$\gamma(\bar{T}g) \equiv \text{Appendix C, Figure C-1} \qquad (34)$$

Applying the $\bar{U}exh$ correction factor = 2.22 and the identities $\mu(\bar{T}g)$, $C_p(\bar{T}g)$ defined above to pipe flow equation (29) yields:

$$h_D = 2.22(.023)(.247+.243\times10^{-4}\bar{T}g)(1.441\times10^{-7}\bar{T}g^{.7})(3600sec/hr)* [(2116.224\ lbf/ft^2\text{-}atm\ P\ \bar{U}exp)/(1.441\times10^{-7}\bar{T}g^{.7}RTg)]^{.8}* B^{-.2}Pr^{-2/3}$$

which simplifies at known R_{cp}, $\bar{U}exp$ values to:

$$h_{D_{BTU/hr\text{-}ft^2\text{-}^\circ R}} = 14.835[2.47 + 2.43\times10^{-4}Tg]\ \frac{135.9\ P}{B^{.2}Tg^{.66}}\ Pr^{-2/3} \qquad (35)$$

From Appendix A; P = 1.05 atm and $2344.58^\circ R \triangleq \bar{T}g \triangleq 2439.06^\circ R$ (TDC to BDC)

through the exhaust stroke. A comparison of $\bar{h}$ calculated from equation (35) and Woschni's exhaust stroke correlation equation (18e) follows:

crank angle	$\bar{T}g$ °R(°K)	$\gamma(\bar{T}g)$ eq.(34)	$Pr(\gamma)$ eq.(33)	$\bar{h}_e$ eq.(18e)	$\bar{h}_D$ eq.(35)
BDC	2439.06 (1355)	1.275	0.698	17.587	17.062
TDC	2344.58 (1303)	1.280	0.701	17.959	17.331

$\bar{h}$ in $BTU/hr\text{-}ft^2\text{-}^\circ R$

The above series of calculations suggest that to a first approximation, application of Woschni's correlation in determining forced convective heat transfer loss for the New Cycle Engine expansion is valid.

CHAPTER THREE

CALCULATION OF UNCORRECTED HEAT TRANSFER LOSS/HEAT RELEASE PER CYCLE, ℜ

Table 3.1 summarizes the calculation of total instantaneous heat transfer rate, $\dot{Q}$, through a complete 360° firing cycle of the New Cycle Engine expansion cylinder using Woschni's correlation for $\bar{h}_e$. For calculation of $\bar{h}_e$ in combustion, motoring P_o is generated graphically in Appendix A, Figure A-1:

$$\dot{Q}_{BTU/sec} = \bar{h}_e A_{HT} (\bar{T}g - \bar{T}w)(1\ hr/3600\ sec) \quad (36)$$

Due to the establishment in preliminary design of a simple cylinder geometry, A_{HT} as a function of crank angle may be determined directly from instantaneous V values; defining instantaneous gas volume height as L_θ and neglecting cylinder sleeve clearance:

$$V = \frac{\pi B^2}{4} L_\theta$$

$$A_{HT} = \frac{2\pi B^2}{4} + \pi B L_\theta = \frac{2\pi B^2}{4} + \pi D[4V/\pi B^2]$$

which at B = 1.22204 ft:

$$A_{HT_{ft^2}} = 2.346 + 3.273[V] \quad (37)$$

The distribution of $\bar{h}_e$ and $\dot{Q}$ as a function of crank angle is plotted in Figure 3-1. It is immediately clear studying the $\bar{h}_e$ distribution over the combustion stroke 55° to BDC, that Woschni's correlation fails to correctly extrapolate luminous

flame radiant heat transfer loss to low r_c operating conditions. No increase in $\bar{h}_e$ occurs due to the predominant influence of increased temperature: associated gas layer ρ decrease and μ increase overcome the effect of K increase, thus lowering $\bar{h}_e$, modeled by laws of similarity solely on forced convective heat transfer. The low r_c and delayed fuel injection operating conditions effectively eliminate any remarkable pressure rise in the cylinder, already at 45° down-stroke at ignition start. Recalling Woschni's coupling of radiant heat transfer in combustion to $C_2(P-P_o)^{.8}$, the desired "lumped form" term effectively disappears.

Uncorrected total heat transfer loss per cycle, Q_T, is determined by numerical integration under the $\dot{Q}$ curve using Simpson's rule:

$$Q_{T_{BTU/cycle}} = \frac{.0010184}{3}[\dot{Q}_{BDC} + 4\dot{Q}_{185°} + 2\dot{Q}_{190°} + \ldots + 2\dot{Q}_{170°} + 4\dot{Q}_{175°} + \dot{Q}_{BDC}] \qquad (38)$$

$$= \frac{.0010184}{3}[7141.613] = 2.42434 \text{ BTU/cycle}$$

From Table 2-2, total charge mass per cycle equals .024537 lbm. At known specific heat release per cycle, Δ heat, equal to 500 BTU/lbm charge, the ratio of total heat transfer loss/heat release per cycle, R_T, equals:

$$R_{T_{uncorrected}} = \frac{2.42434 \text{ BTU}}{(500\text{BTU/lbm})(.024537 \text{ lbm/cycle})}$$

$$= 19.761\%$$

The inability of Woshni's correlation to account for radiant heat transfer in low r_c operation is clearly demonstrated by repeating the numerical integration with the combustion term in equation (18d) eliminated ($C_2 = 0$):

Simpson's Multiplier = 7038.088

Q_T = 2.3892 BTU/cycle

$\eta_{T_{uncorrected}}$ = 19.474%

Considering the accuracy of the correlation in general, for preliminary design prediction purposes setting $C_2 = 0$ is considered valid.

To correct for luminous flame radiation heat transfer loss, a value of $\overline{q_W/q_{NCE}}$ radiation must be determined which, in comparison of $\overline{q_W/q_{NCE}}$ forced convection calculated in Chapter Two, will allow first approximation of the required η_T correction factor. As there exists no theoretical basis for coupling magnitude of luminous flame radiation to $(P-P_o)^{.8}$, an attempt to determine the desired ratio from $(P-P_o)^{.8}$ profiles must be disregarded in favor of calculation founded on known principles of radiation heat transfer in diffusion flame combustion.

TABLE 3-1

Calculation of New Cycle Engine expansion cylinder firing cycle $\dot{Q}$ using Woschni's correlation at 5° crank angle increments

crank angle θ°	$\bar{h}_e$ $\frac{BTU}{hr\text{-}ft^2\text{-}^\circ R}$	A_{HT} ft^2	$\bar{T}g-\bar{T}w$ $^\circ R$	$\dot{Q}$ $\frac{BTU}{sec}$
	eq(18)	eq(37)	$\bar{T}w=900^\circ R$	eq(36)
charge induction	equation (18c)			
5	16.944	2.357	1249.04	13.856
10	20.191	2.390	1259.25	16.878
16	24.006	2.445	1295.73	21.128
20	28.209	2.522	1325.26	26.190
25	32.029	2.618	1329.71	30.972
30	34.236	2.734	1294.29	33.652
35	33.888	2.867	1216.61	32.834
40	31.168	3.017	1110.57	29.009
45	27.164	3.181	996.6	23.924
combustion-expansion	equation(18d)			
50	26.086	3.358	1351.6	32.888
55	23.969	3.548	1671.21	39.445
60	22.066	3.741	1964.13	45.038
65	20.853	3.944	2236.02	51.083
70	18.710	4.152	2164.15	46.700

TABLE 3-1 (CONT'D)

crank angle θ°	$\bar{h}_e$ $\frac{BTU}{hr\text{-}ft^2\text{-}^\circ R}$	A_{HT} ft^2	$\bar{T}g-\bar{T}w$ $^\circ R$	$\dot{Q}$ $\frac{BTU}{sec}$
75	17.084	4.362	2098.73	43.444
80	15.742	4.573	2039.11	40.775
85	14.632	4.783	1984.75	38.584
90	13.715	4.990	1935.18	36.789
95	12.841	5.192	1889.98	35.002
100	12.099	5.388	1848.18	33.478
105	11.457	5.577	1811.25	32.148
110	10.865	5.757	1777.09	30.877
115	10.438	5.927	1746.03	30.006
120	10.015	6.087	1717.83	29.089
125	9.652	6.236	1692.29	28.361
130	9.329	6.373	1669.22	27.567
135	9.052	6.498	1648.44	26.934
140	8.830	6.611	1629.82	26.428
145	8.632	6.711	1613.21	25.959
150	8.467	6.797	1598.51	25.554
155	8.334	6.871	1585.62	25.221
160	8.229	6.930	1574.46	24.941
165	8.151	6.978	1564.96	24.725
170	8.086	7.011	1557.07	24.517
175	8.044	7.031	1550.74	24.363
BDC	8.028	7.037	1545.46	24.260

TABLE 3-1 (CONT'D)

crank angle θ°	F_e $\frac{BTU}{hr\text{-}ft^2\text{-}^\circ R}$	A_{HT} ft^2	$T_g - T_w$ $^\circ R$	$\dot{Q}$ $\frac{BTU}{sec}$
exhaust	equation (18e)			
BDC	17.587	7.037	1539.06	52.909
185	17.604	7.031	1534.63	52.763
190	17.619	7.011	1530.70	52.523
195	17.634	6.978	1526.81	52.187
200	17.649	6.930	1522.95	51.741
205	17.664	6.870	1519.13	51.208
210	17.678	6.797	1515.36	50.578
215	17.693	6.710	1511.61	49.894
220	17.707	6.611	1507.99	49.035
225	17.721	6.498	1504.41	48.121
230	17.736	6.373	1500.90	47.125
235	17.748	6.236	1497.47	46.037
240	17.761	6.087	1497.47	44.870
245	17.774	5.927	1490.89	43.628
250	17.786	5.756	1487.75	42.308
255	17.798	5.576	1484.71	40.929
260	17.810	5.388	1481.71	39.498
265	17.821	5.192	1478.95	38.012
270	17.832	4.990	1476.24	36.488
275	17.842	4.783	1473.65	34.933
280	17.852	4.573	1471.18	33.362

TABLE 3-1 (CONT'D)

crank angle θ°	$\bar{h}_e$ $\frac{BTU}{hr\text{-}ft^2\text{-}^\circ R}$	A_{HT} ft^2	$T_g - T_w$ $^\circ R$	$\dot{Q}$ $\frac{BTU}{sec}$
285	17.861	4.362	1468.82	31.786
290	17.870	4.152	1466.58	30.226
295	17.879	3.944	1464.46	28.685
300	17.887	3.741	1462.44	27.198
305	17.895	3.545	1460.54	25.737
310	17.902	3.356	1458.73	24.346
315	17.909	3.181	1457.03	23.057
320	17.915	3.017	1455.41	21.851
325	17.921	2.867	1453.88	20.750
330	17.927	2.734	1452.41	19.774
335	17.933	2.618	1451.01	18.923
340	17.938	2.522	1449.67	18.217
345	17.944	2.445	1448.36	17.651
350	17.949	2.390	1447.09	17.244
355	17.954	2.357	1445.83	16.996
TDC	17.959	2.346	1444.58	16.906

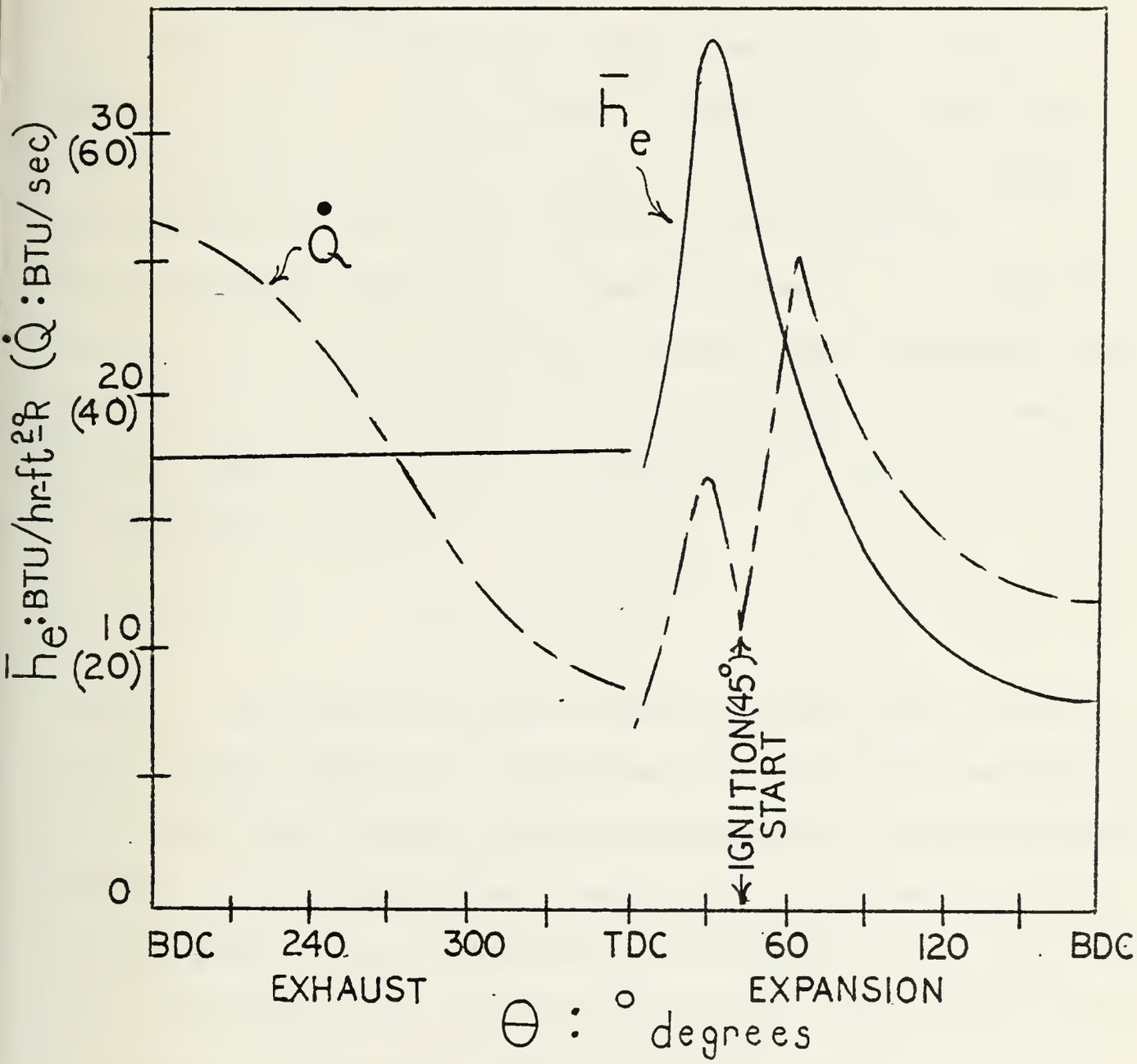

FIGURE 3-1: Expansion cylinder firing cycle $\bar{h}_e$ and $\dot{Q}$ versus crank angle; Woschni's coorelation

CHAPTER FOUR

RADIANT HEAT TRANSFER IN THE NEW CYCLE ENGINE EXPANSION CYLINDER

1. THEORETICAL BACKGROUND

When a temperature difference exists between two bodies, part of the thermal energy is transferred as electromagnetic waves of radiation at varying wavelengths, λ, characteristic of the body temperature and identity. In the electromagnetic spectrum, thermal energy is propagated through .01 $\mu m \leq \lambda \leq 100\ \mu m$. Bodies above absolute zero temperature continuously emit energy which, when striking another body, may be partly absorbed, α, reflected, ρ, or transmitted , τ, where:

$$\alpha + \rho + \tau = 1 \qquad (39)$$

Thermal radiation reflected from and transmitted through a body is again absorbed, reflected by, or transmitted through any additional bodies ultimately establishing an equilibrium state. An ideal body that absorbs all radiation is known as a black body; if no radiation is transmitted, as in the case for most industrial liquids and materials, the body is known as opaque. Combustion chambers covered with a thin film of oil contaminated with soot particles will absorb a significant percentage of incident radiation, $\tau = 0$.

Thermal energy emitted from a body unit surface per unit time at a particular wavelength, the monochromatic

emissive power, E_λ, can be determined as a function of temperature T(°K) by Planck's Law:

$$E_{\lambda\ erg/sec-cm^3} = 2\pi c c_p{}^2 \lambda^{-5} [c c_p / e^{c_b \lambda T} - 1]^{-1} \qquad (40)$$

where: c = speed of light 2.997902×10^{10} cm/sec

c_p = Planck's constant 6.623777×10^{-27} erg-sec

c_b = Boltzmann's constant 1.38026×10^{-16} erg/°K

λ = wavelength in cm

T = temperature in °K

E_λ will increase with increasing λ to a maximum value then decreases, the distribution shifting toward the shorter wavelengths at higher body temperatures. The relationship between T(°K) and λ_{max} is determined by Wein's Law of Displacement:

$$\lambda_{max}\ T(°K) = 2898\ cm-°K$$

The total radiant emissive power, E, may therefore be calculated at a given body temperature by integrating the area under the curve:

$$E = \int_0^\infty E_\lambda\ d\lambda \qquad (41)$$

For a given black body, substitution of equation (40) into equation (41) yields the Stephan Boltzmann Law:

$$E_{\substack{Black\ Body \\ BTU/hr-ft^2}} = \sigma_o T^4\ (°R) \qquad (42)$$

where: σ_o = Stephan Boltzmann constant 1.713×10^{-9} BTU/hr-ft^2°R^4

Real bodies, however, are not absolutely black. Those bodies of a continuous radiating electromagnetic spectrum where the E_λ curve is proportional to that of an absolute black body at each λ are known as grey bodies. The ratio of emissive power of a grey body to an absolute black body is known as the coefficient of emissivity, ε:

$$\frac{E \text{ grey body } (T)}{E \text{ black body } (T)} = \varepsilon \qquad (43)$$

From an analysis of equilibrium emittance and absorptance between a grey body and its surroundings at the trivial case of each equal to the same temperature, it can be demonstrated that ε is equal to α (Kirchoff's Law). This important phenomenon, strictly correct only within the defined limitations, is fortunately observed to be approximately correct in many real conditions where temperature differences are not severe. Additionally, many real industrial materials radiate near grey at very high values of α; instantaneous radiant heat transfer rate, $\dot{Q}_R$, between two near-grey bodies 1 and 2 of different temperatures at a distance apart may therefore be calculated from equation (44):

$$\dot{Q}_{R1,2\ \text{Btu/sec}} = \varepsilon_{1,2}\sigma_o F_{1,2} A_{HT} (T_1^4 - T_2^4)(1 \text{ hr}/3600 \text{ sec}) \qquad (44)$$

where: $\varepsilon_{1,2} = \dfrac{1}{\frac{1}{\varepsilon_1} + \frac{1}{\varepsilon_2} - 1}$

$F_{1,2}$ = geometric view factor between bodies 1 and 2

Tables providing formulas for ε and F calculation between multiple bodies at various common geometries are published in standard heat transfer texts. For gas or incandescent solid particles radiating as a defined unit body within an encompassing simple geometry combustion cylinder, F may be assumed equal to unity.

2. NON-LUMINOUS GAS RADIATION

2.1 CHARACTERISTIC HEAT TRANSFER EQUATIONS

Unlike solid bodies which radiate across continuous wavelength spectrums, gases emit and absorb energy at direct wavelengths only in line spectra. For simple monatomic and diatomic gases such as O_2,N_2, and H_2, the line spectra are negligible and may be considered transparent (τ = 1). For complex gases such as generated in exhaust products, however, radiant capacity may be significant. CO_2 and H_2O vapor predominate as radiant emitting gases in combustion products; the significant bands of radiation are [14]:

	CO_2	H_2O
Band 1	2.36 - 3.02 μm	2.24 - 3.27 μm
Band 2	4.01 - 4.80 μm	4.8 - 8.5 μm
Band 3	12.5 - 16.5 μm	12 - 25 μm

In radiating gas, both emittance and absorptance exist throughout the gas volume. Penetrating radiant energy will be reduced by absorption proportional to the number of molecules in the ray path as a direct function of individual gas partial pressure, temperature, and path length, X. This intensity attenuation is expressed by Beers Law:

$$\alpha_\lambda = 1-\exp(k_\lambda X) \qquad (45)$$

where: k_λ = monochromatic absorption coefficient per unit length

X = radiant path length

A gas volume is, of course, not grey. For ease of calculation an equivalent gas emissivity, ε_g, is defined in accordance with equation (46):

$$\varepsilon_g = 1 - \exp(k_g l_R) \qquad (46)$$

where: k_g = apparent gas absorption coefficient per unit length

l_R = effective mean beam length

For a defined gas volume of V and boundary surface A_{HT}, l_R may be determined from equation (47):

$$l_{R_{ft}} = \frac{3.4V}{A_{HT}} \qquad (47)$$

$\dot{Q}_R$ between the gas and surrounding wall of emissivity ε_w may then be determined from equation (48):

$$\dot{Q}_{R_{BTU/sec}} = \varepsilon_g \varepsilon_w \sigma_o A_{HT} [\bar{T}g^4 - \bar{T}w^4](1\ hr/3600\ sec) \qquad (48)$$

For gas volumes containing more than one radiating gas, total ε_g is calculated by addition of individual gas emissivities and an additional negative correction factor, $-\Delta\varepsilon_g$, for radiant band coincidence which reduces the sum. For internal combustion engine exhaust gas products from hydrocarbon

based fuels, the resultant total gas emissivity may be considered equal to:

$$\varepsilon_g = \varepsilon_{CO_2} + \varepsilon_{H_2O} - \Delta\varepsilon_g \qquad (49)$$

Again, significant data base has allowed development of graphs for ε_{CO_2}, ε_{H_2O}, and $-\Delta\varepsilon_g$ as a function of P, $\bar{T}g$ and l_R, and are published in standard heat transfer texts. Empirical formulas based on experimental data for calculation of emissive power of CO_2 and H_2O vapor useful for a first approximation in U.S. units are [14]:

$$E_{CO_2} \underset{BTU/sec\text{-}ft^2}{} = 1.7125\times10^{-5}(P_{CO_2} l_R)^{1/3}(\bar{T}g/100)^{3.5} \qquad (50)$$

$$E_{H_2O} \underset{BTU/sec\text{-}ft^2}{} = 1.6738\times10^{-5}\, P_{H_2O}{}^{.8} l_R{}^{.6}(\bar{T}g/100)^{3.0} \qquad (51)$$

2.2 PREDICTION OF GAS RADIATION HEAT TRANSFER

References [3, 6, 8, 9, 10, 14, 15, 16] state that gas radiation is insignificant in calculating high r_c CI engine heat transfer loss. To ascertain if separate consideration of gas radiation in the low r_c New Cycle Engine expansion cylinder may be required, it is sufficient to estimate $\dot{Q}_R$ magnitude at maximum l_R and $\bar{T}g$ in the exhaust stroke and compare to $\dot{Q}$ calculated by Woschni's correlation. For a typical diesel fuel of C/H mass ratio equal to 6 operating at lean Φ, distribution of combustion product gas includes approximately 10% CO_2 and 10% H_2O water vapor [14].

Calculation of $\dot{Q}_R$ using equation (48) and (49) at Appendix A parameter values at exhaust stroke BDC follows:

$\dot{Q}$ Woschni = 52.909 BTU/sec

$V = 1.43333\ ft^3$

$A_{HT} = 7.037\ ft^2$

$\bar{T}g = 2439.06°R$

P = 1.05 atm: $P_{H_2O} = .105$ atm $\quad P_{CO_2} = .105$ atm

$$l_R = \frac{3.4(1.43333)}{7.037} = .6925 \text{ ft}$$

$$\dot{Q}_{CO_2} \approx (1.7125\times10^{-5})[(.105)(.6925)]^{1/3}\left(\frac{2439.06}{100}\right)^{3.5}(7.037)$$

$$= 3.604 \text{ BTU/sec}$$

$$\dot{Q}_{H_2O} \approx (1.6738\times10^{-5})(.105)^{.8}(.6925)^{.6}\left(\frac{2439.06}{100}\right)^{3.0}(7.037)$$

$$= 0.226 \text{ BTU/sec}$$

$$\dot{Q}_{R_{\underline{gas}}} \approx 3.830 \text{ BTU/sec}$$

In the above calculations, corrections for $\Delta\varepsilon_g$, ε_w, and emissive power of the cylinder surface proportional to $\sigma_o\bar{T}w^4$, all which would reduce the total, have been ignored. The estimated value equal to 3.83 BTU/sec is well absorbed into 52.909 BTU/sec. Noting that for all other crank angles in the exhaust stroke both $\bar{T}g$ an l_R decrease, plus in the combustion-expansion stroke luminous flame radiation exists, it may be assumed that separate consideration of gas radiation in the New Cycle Engine expansion cylinder heat transfer calculation is not required.

3. LUMINOUS FLAME RADIATION

3.1 FUNDAMENTAL CAUSE

The phenomenon of flame radiation is quite complex, dependant intimately on the physical and chemical properties of combustion, pressure, temperature, and a myriad of engine and fuel parameter variables. Two basic flame types are produced with respect to radiant capacity: non-luminous flame characteristic of SI engines, and luminous flame characteristic of CI engine diffusion flames. In SI engines, pre-mixed fuel and air are adiabatically heated in compression then ignited by a spark resulting in combustion by turbulent propagation of flame through the charge from the point of ignition. The mixture burned at the beginning of flame travel expands, then recompresses, reaching temperatures hundreds of degrees higher than that which is burned last. This recompression of combustion product gases, particularly CO_2, yields visible yellow radiation. No intermediate solid particles are formed, however, and apparent emissivities of combustion product gases as a function of near transparent λ bands is small. The driving potential for radiant heat transfer, proportional to T^4, diminishes more rapidly then forced convection heat transfer proportional to T; the contribution of instantaneous radiant heat transfer, $\dot{Q}_R$, integrated over the engine cycle is insignificant.

In CI engines, the fuel spray injecting into adiabatically compressed air near piston TDC is ignited by

spontaneous explosion of a micro-mixture of fuel and entrained air, thereafter burning diffusively. There are many sources of ignition and flame tends to conform to the fuel spray shape until dispersed by gas motion. In the chemical combustion of hydrocarbon based fuels, cracking to simpler structures and polymerization occurs. When insufficient local O_2 exists to feed the rapidly increasing reactivity of the mixture, thermal decomposition of C-H and C-C bonds occurs resulting in incandescent carbon soot formation radiating in a continuous spectrum. Alcock et al [11], in a classic high speed photographics study of a Meurer direct injection, medium speed CI engine, clearly observes a luminous flame front filling the chamber within 20° of ignition start (10° BTDC), glowing white hot at peak flame temperatures equal to 4500°R, then cooling by expansion to dull red. Unlike SI engines where combustion completes early in the expansion stroke, the CI combustion process extends late into the expansion stroke.

This difference between local O_2 concentration and cracking rate is the principle cause of soot formation and luminous flame radiation. The magnitude of associated heat transfer cannot be ignored, and has been measured by Annand [3], Sitkei [14], Dent et al [10], Flynn et al [15], and Oguri et al [8] as typically 20% to 30% of total heat transfer loss, Q_T , in non-swirl enhanced four stroke, direct injection, high r_c CI engines under varying design and operational conditions. Oguri et al [8] demonstrate this in

Figure 4-1, showing Q_R/Q_T between two such different size CI engines operating at varying RPM, load, and cylinder wall soot contamination: Engine A is a 5.9 inch bore natural aspirating engine; Engine B is a 12.2 inch bore supercharged engine. In very large diesel engines the contribution to Q_T of radiant heat transfer is even greater; J. Butler of Dexford Co., United Kingdom, estimated the radiant component of Q_T as 75% for a 40 inch bore diesel [8]. In any case, measured peak flame emissivities, ε_f, approaches unity (1.0), and while reaction zone temperature is difficult to determine, a consensus opinion shared is that peak radiant temperature is much higher than $\bar{T}g$. Chapman et al state [17, pg 13]:

> "the apparent radiant temperature is much closer to the flame temperature than the average bulk gas temperature."

Peak flame temperature, T_f, reached in high r_c CI engines is typically 4200 ± 200°R.

3.2 KHAN ET AL COMBUSTION SOOT PRODUCTION MODEL

While a valid quantitative calculation of soot concentration in New Cycle Engine combustion is not possible, a brief study of a soot production model for a simple design, direct injection, quiescent CI engine will illustrate the critical parameters on which soot formation is based and establish a foundation for empirical estimation of peak New Cycle Engine $\dot{Q}_R$. Khan et al [18] have developed semi-empirical equations for soot formation in a fuel jet mixing model applied successfully to a 9.8 cm bore engine at

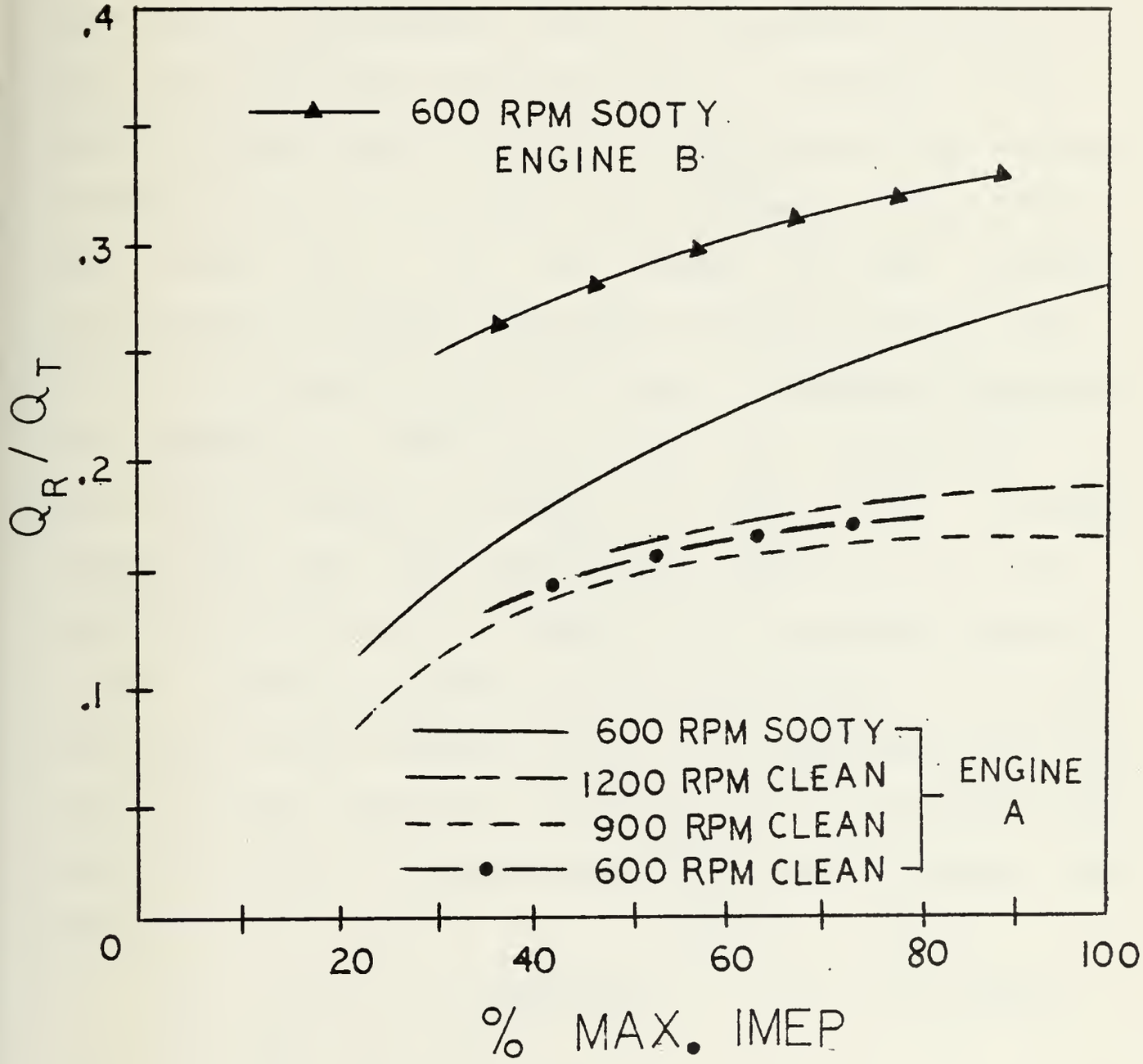

FIGURE 4-1: Q_R/Q_T for two 4 stroke, direct injection CI engines under varying operating conditions as observed by Oguri et al [8]

2000 RPM. This simple model ignores complex stratification and consideration of fuel droplet evaporation; all unburnt fuel is assumed to be in the vapor state. The jet mixing model injecting into a cross-stream air flow is shown in Figure 4-2. The air entrainment zone (e) is composed of a fuel rich zone (c) where soot formation occurs, a products zone (d) where intense reaction occurs, and an outer zone composed primarily of air. Outside the entrainment zone is the air mass zone (a). For the purpose of soot formation calculations, a local equivalence ratio of unburnt fuel in the fuel rich zone, Φ_u, is defined. A series of equations are proposed by Khan et al for Φ_u calculation; the significant points of which is that Φ_u is inversely proportional to air entrainment which is in turn a progressive function of air swirl ratio and engine speed. Φ_u is not, however, directly coupled to Φ charge. The overall mechanism of soot formation under high temperature and short reaction time conditions characteristic of diffusion flame combustion may be characterized by an Arrhenius type equation:

$$\frac{d\mathcal{S}}{dt} = c_s \frac{V_u}{V} \Phi_u^{3} P_u e^{-E_s/R_o T_u} \qquad (52)$$

where: $\frac{d\mathcal{S}}{dt}$ = soot formation rate
V_u = volume of soot formation zone (c)
V = cylinder volume
P_u = partial pressure of unburnt fuel in soot formation zone (c)
T_u = local temperature of soot formation zone (c)
c_s = soot formation rate coefficient
E_s = soot combustion activation energy
R_o = universal gas constant

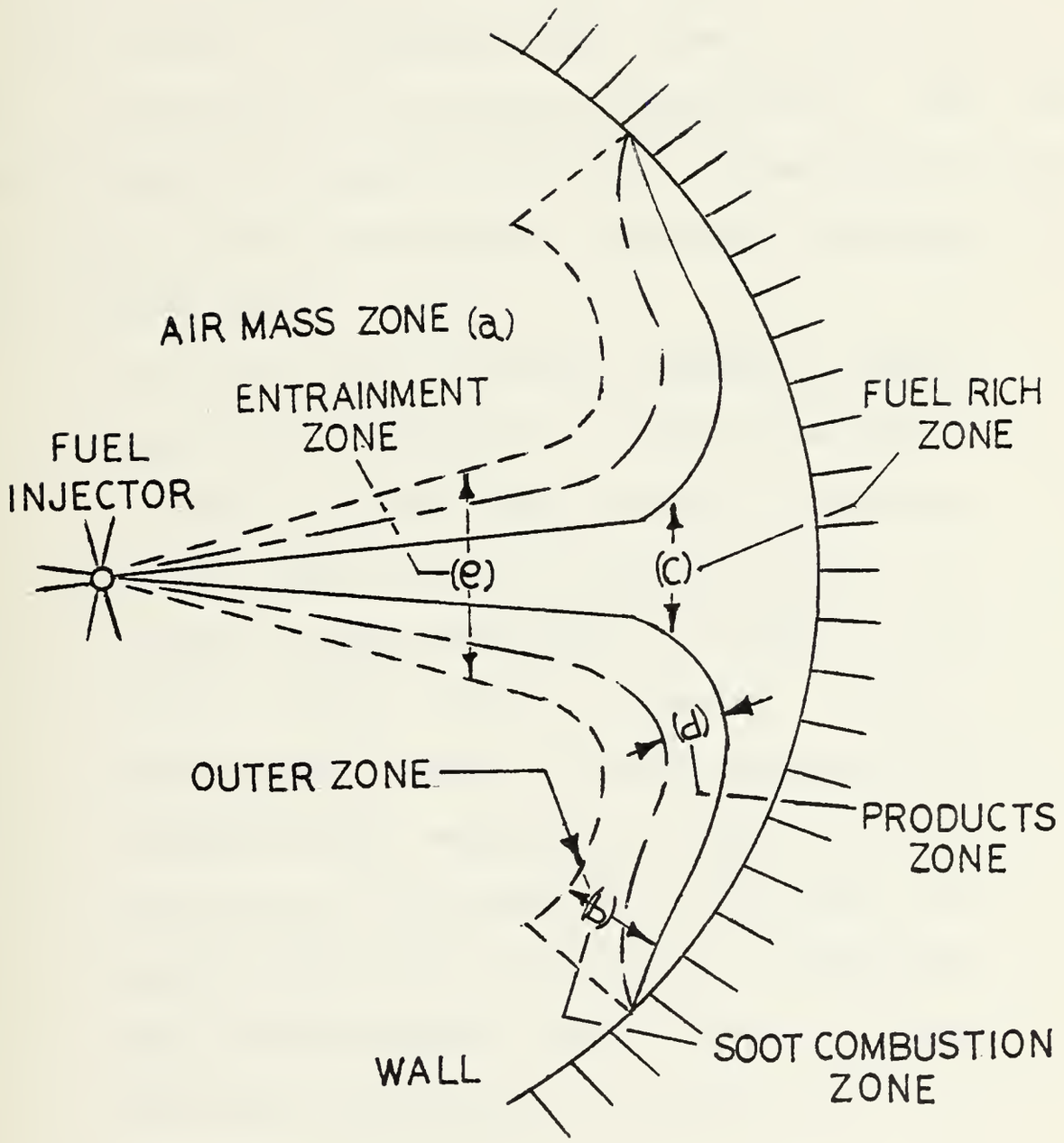

FIGURE 4-2: Soot production fuel jet mixing model of Khan et al [18]

After formation, soot particles coagulate and/or combust from a typical initial diameter of 250 Å where combustion of soot coagulate is again controlled by an Arrhenius type equation proportional to the partial pressure of O_2.

The values of constants and coefficients are, of course, a function of individual engine design and fuel structure selected to best "curve fit" experimental data. Valuable qualitative conclusions, however, stand out from the work by Khan et al:

1. The rate of soot formation depends on three principle parameters: local P (partial), T, and Φ in the fuel rich soot formation zone. The effect of varying overall Φ charge is moderated as Φ_u is always near unity. Swirl ratio, however, has a significant effect. A comparison of soot concentrations measured by Khan et al, Flynn et al, and Dent et al is shown in Figure 4-3 which graphically illustrates soot concentration, thus luminous flame radiation, suppression in high swirl CI engines.
2. Approximately 60%, as measured by Khan et al [18], of soot initially formed is burnt as it moves from the cooler fuel rich zone (c) into the products zone (d) where soot oxidation incandescent radiant emission is

a grey body, optically thick. The exhausted soot is that portion which escapes the high temperature products reaction zone (d) in the process of turbulent diffusion from the fuel rich to the lean zone.

3. High speed photography indicates that the majority of soot formation occurs at the beginning of the main combustion phase, within an extremely short period [see Figure 4-3]. The total amount of soot remains constant in the later combustion stages.

A clear conclusion of this model is that both soot formation rate and soot combustion rate are progressive functions of fuel and O_2 partial pressures. The New Cycle Engine, operating at significantly reduced expansion cylinder pressures, should therefore experience a marked reduction in luminous flame radiant heat transfer. Due to lack of (built) engine test data however, the degree to which Q_R decreases relative to magnitudes observed in high r_c CI engines must be estimated from indirect empirical relationships. The quality of this estimation, based principly on reduced pressure consideration in low swirl conditions, must be tempered with the knowledge that many other operating parameters have a secondary effect on flame emissivity and temperature.

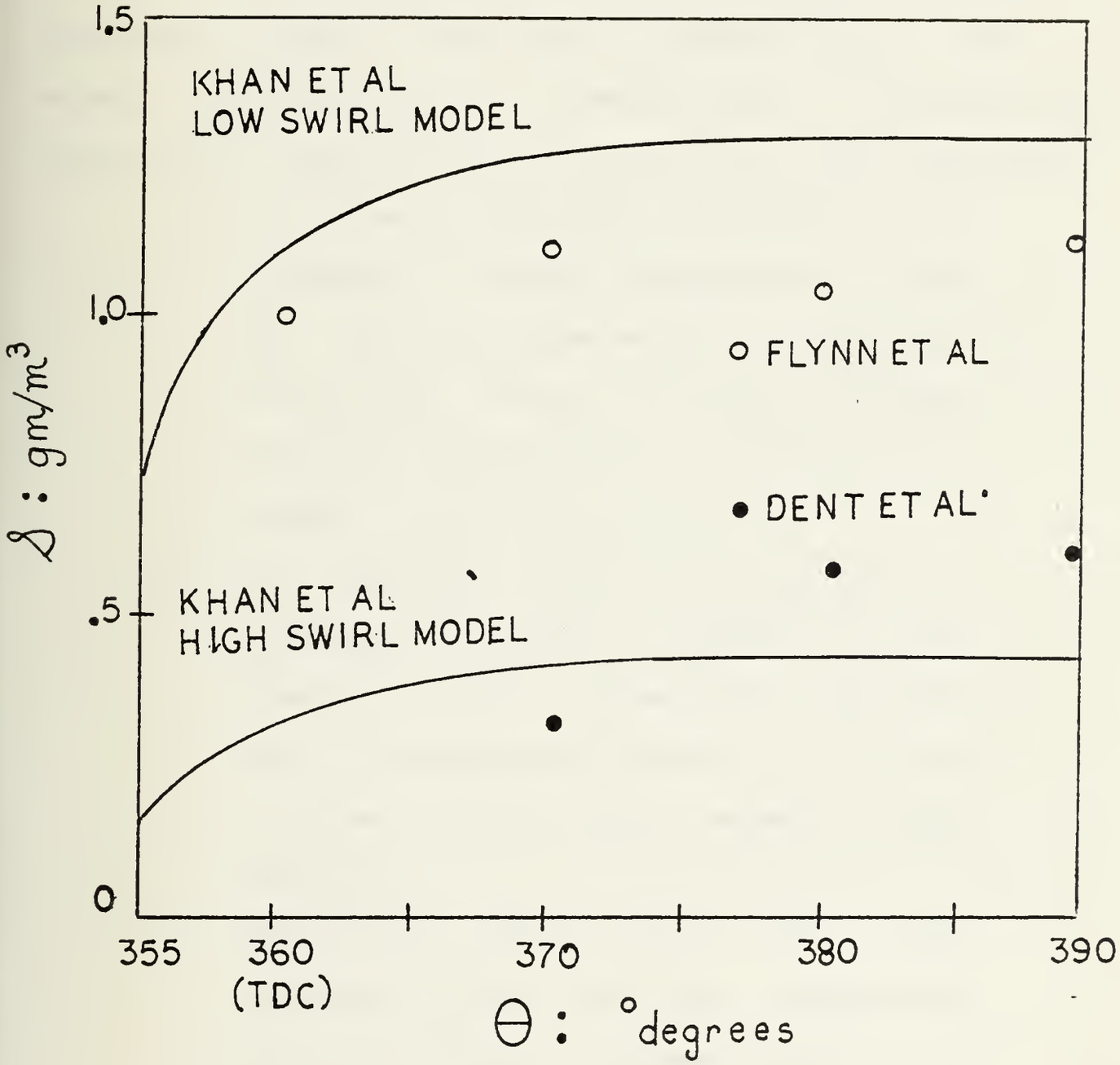

FIGURE 4-3: Comparison of in-cylinder soot conentration, δ, versus crank angle as observed by various investigators [10]

3.3 SECONDARY FACTORS AFFECTING COMBUSTION SOOT CONCENTRATION

Extensive tests performed by Flynn et al on a four stroke, direct injection CI engine, with piston cup combustion chamber enlarged to suppress swirl ratio and enhance soot production, illuminate many of these secondary effects; the important ones of which are listed below [16]:

1. Q_R increased with inlet manifold pressure increase at nearly proportional rate; much less ignition delay and fuel/air pre-mixing occurs causing increased tendency for soot formation in diffusion flame.
2. As injection time was advanced an increase in $\bar{T}g$ and an increase in peak apparent radiant temperature occurred; due to fourth power effect a significant increase in peak radiant emissive power results.
3. Decreasing cetane number with fixed reference fuel families encouraged ignition delay, increased fuel/air pre-mixing, and reduced soot formation; at supercharged operation this effect is effectively suppressed due to predominant effect of manifold pressure on ignition delay.

4. Increasing C/H mass ratio fuels at fixed cetane numbers encouraged Q_R due to simple availability of carbon concentration; the rate is not proportional to C/H mass ratio and apparent only at high ratio aromatic fuels.

Flynn et al additionally note that the apparent flame optical thickness, $k_f l_R$, diminishes approximately in inverse proportion to increasing cylinder volume. This conforms with the Khan et al model and Figure 4-3, indicating that the number of incandescent radiating particles in later combustion stages is essentially constant.

3.4 CHARACTERISTIC HEAT TRANSFER EQUATIONS

Emission as a function of wavelength for clouds of small particles obeys a variation described by equation (53):

$$E_\lambda = 1 - \exp(-k_\lambda l_R / \lambda^{.95}) \qquad (53)$$

The spectrum is near grey, and for simplicity of calculation can be converted to equivalent grey body emissivity:

$$\varepsilon_f = \frac{\int_{\lambda_o}^{\lambda_n} \varepsilon_\lambda q_\lambda d\lambda}{\int_{\lambda_o}^{\lambda_n} q_\lambda \delta\lambda} \qquad (54)$$

where: $\lambda_o - \lambda_n$ is range of significant λ band

The effect of combustion cylinder wall reflectivity, ξ_w, as demonstrated by Oguri et al in Figure 4-1, may be corrected

for by determination of an apparent flame emissivity, ε_a, according to equation (55):

$$\varepsilon_a = \frac{(1-\bar{\xi}_w)\varepsilon_f}{1-\bar{\xi}_w\varepsilon_f} = 1 - e^{-k_f l_R} \qquad (55)$$

where: k_f = apparent flame absorption coefficient per unit length

When flame envelopes the entire cylinder volume, observed by Alcock et al [11] to occur approximately 10 to 20° after ignition start, l_R may be calculated by equation (47) as a function of instantaneous cylinder V and A_{HT}. Sitkei et al [15] state that surfaces of pre-swirl chambers, piston crown and cylinder heads have $\bar{\xi}_w = 0.1$ (approx.); cylinder sleeve $\bar{\xi}_w = 0.2$ (approx.). It should be noted that estimates for $\bar{\xi}_w$ vary greatly, in part due to different modeling of cylinder surfaces as specular reflective to semi-rough diffusive reflective characteristic of oil soaked, soot-contaminated surfaces. $\dot{Q}_R$ may then be determined by equation (56):

$$Q_{R_{f\,BTU/sec}} = \varepsilon_a \sigma_o A_{HT}[T_f^4 - \bar{T}_w^4](1\ hr/3600\ sec) \qquad (56)$$

3.5 SITKEI ET AL METHOD OF APPARENT FLAME EMISSIVITY, ε_a, CALCULATION

A useful empirical relationship used by Annand [3] and Dent et al [10] based on known soot concentration is stated in equation (57) in U.S. units:

$$k_f = 5898\ \mathcal{S}\ ft^{-1} \qquad (57)$$

where: $\mathcal{S}$ = soot concentrations in lbm/ft^3

For estimation of ε_a without knowledge of soot concentration, Sitkei et al propose the following definition of ε_a as a function of instantaneous P, Φ, l_R and crank angle past ignition start [15]:

$$\varepsilon_a = \varepsilon_o \left[1 - e^{-.3048 k_p P l_R}\right] \qquad (58)$$

where: ε_o = emissivity of infinitely thick radiating flame; ≈ 0.8

k_p = apparent flame absorption coefficient per unit length-unit pressure (atm)

Values of k_p are determined from Figure 4-4, at applicable crank angle, and excess air factor equivalent to Φ^{-1}. Sitkei et al based Figure 4-4 on measurements conducted by a photo-electric pyrometer unit through a quartz view window insert to a swirl pre-combustion chamber of a four stroke Steyr diesel at r_c equal to 18.5. Recognizing that ε_a is dependant on many additional variations in engine operating parameters, Sitkei states that to a first approximation [14, pg. 56]:

> "in the absence of other data, it is felt that k_p given here is universally adaptable to all engines of the diesel type.... with the known P-V diagram of the engine under test the variation of k_p can be found"

Inherent in this assumption is an assumed $\bar{\xi}_w$ of 10% to 20%, an ignition start near TDC, a rather arbitrary value of ε_o = 0.8 based on observed steady state diesel fuel flame emissivities in combustors, and the belief that ε_a observed in a 2.6 cm pre-combustion chamber may be extrapolated to main cylinder emissivities.

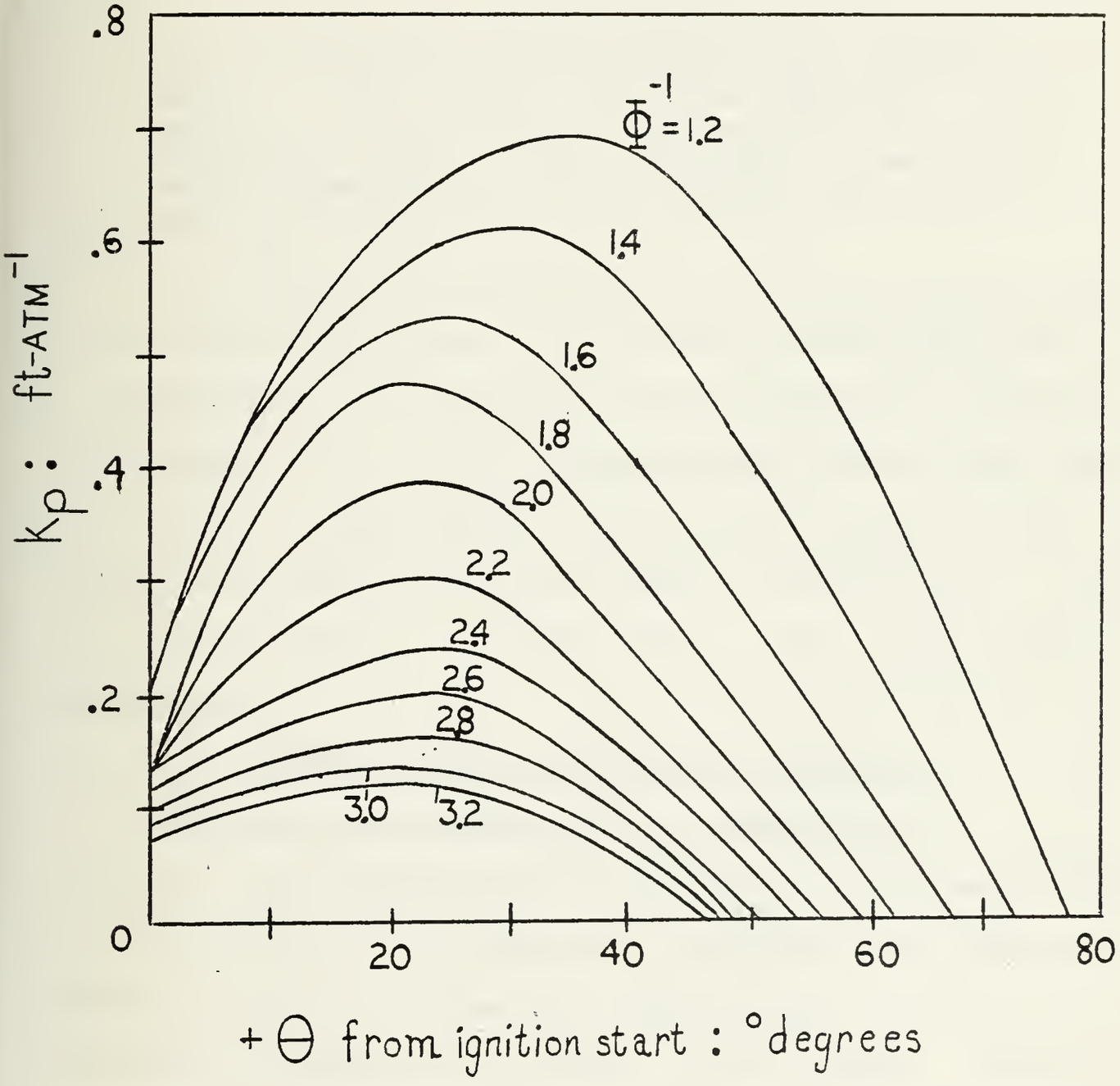

FIGURE 4-4: Variation of k_p versus angular displacement for ξ_a calculation; Sitkei et al model [14]

It should be noted that the values of ε_a determined by the above method are generally less than observed by a number of other investigators in direct injection CI engine testing. Dent et al state [10, p. 1760]:

> "The essential results of Sitkei and Ramanaiah are in agreement with those of Flynn et al in terms of the trend of flame emissivity and optical thickness with crank angle, load, and overall air fuel ratios. However, the magnitude of the flame emissivity and optical thickness are approximately half."

For first approximation of predicted peak ε_a in the New Cycle Engine expansion cylinder, it is therefore believed that the ε_a obtained by the Sitkei et al method should be multiplied by a factor of 2. It is also noted that Sitkei et al agree with typical Q_R/Q_T range of 20% to 30% even at reduced ε_a values due to assumption of Belinskiy's significantly higher T_f profile shown in Figure 4-5, vice direct optical measurement.

3.6 LOW COMBUSTION PRESSURE POWER UNIT METHOD OF APPARENT FLAME EMISSIVITY, ε_a, CALCULATION

For first approximation purposes, an alternate method of predicting ε_a is to examine the characteristic emissivity equations used in power units operating at the low peak combustion pressures of the New Cycle Engine. Different properties, continuous flaming and non-reciprocating mechanics of gas turbines do not allow broad application of flame emission data to internal combustion engines. However, actual combustion kinematics and flame luminosity observed in power units at pressure conditions more reflective of the New

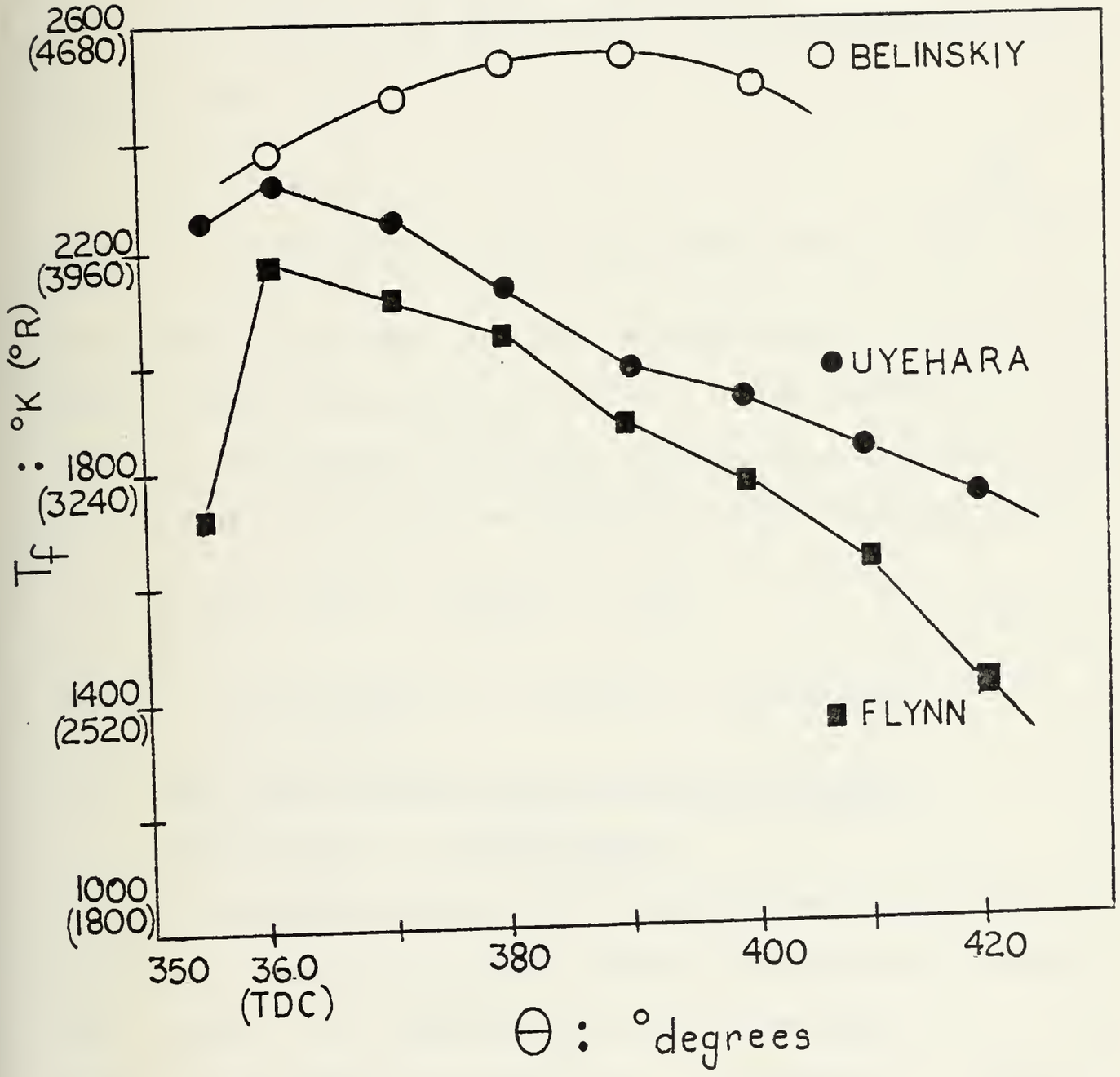

FIGURE 4-5: Measured T_f in CI engines versus crank angle as observed by various investigators [10]

Cycle Engine should not be ignored. It is therefore considered that a fair prediction of New Cycle Engine peak ε_a only can be ascertained by use of gas turbine power unit emissivity equations using diesel fuel properties.

For gas turbine application, ε_a can be determined by equation (59) [19]:

$$\varepsilon_a = 1 - e^{-z} \qquad (59)$$

where: $z = -38636.55\ P[(\text{fuel/air mass ratio})_R]^{.5}\bar{T}g^{-1.5}\mathfrak{L}$

The flame luminosity, $\mathfrak{L}$, can be determined as a function of fuel C/H mass ratio from Figure 4-6. For commercial liquid fuels of conventional character ranging from gasoline to fuel oil, C/H mass ratio can be estimated using equation (60):

$$\frac{C}{H}\ \text{mass ratio} = .16015\rho - 1.66 \qquad (60)$$

where: ρ fuel density in lbm/ft^3 is referenced to 518°R (288°K)

3.7 BOLTZMANN NUMBER FUNCTION METHOD OF FLAME Temperature, T_f, CALCULATION

A consensus opinion of investigators support that for first approximation purposes, radiant temperature is equal to T_f; various T_f profiles published from high r_c CI engine testing are shown in Figure 4-5. An empirical correlation allowing calculation of T_f is the Boltzmann number function, $\bar{T}g/T_f = f\ (Bo^{\#})$, established in Figure 4-7. The $Bo^{\#}$ is defined in accordance with equation (61) [14]:

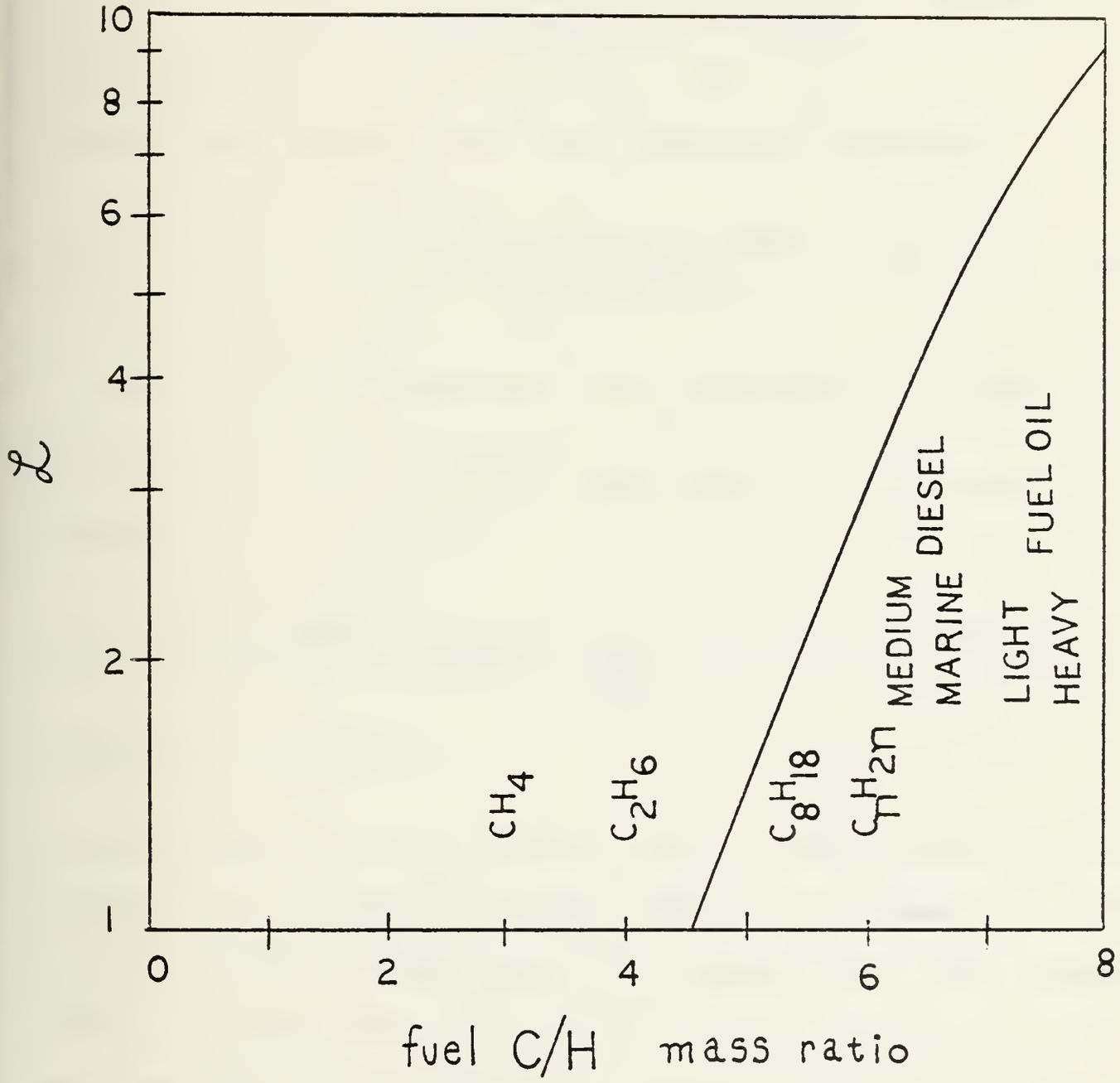

FIGURE 4-6: Flame luminosity, $\mathcal{L}$, as a function of fuel C/H mass ratio in low combustion pressure power units [19]

$$Bo^{\#} = \frac{B_e C_{p\ fuel}}{\sigma_o \varepsilon_f A_{HT} T_f^3} \qquad (61)$$

where: B_e = fuel consumption rate

$C_{p\ fuel}$ = mean total specific heat of combustion products of 1 lbm of fuel

For ease of calculation, B_e and C_p fuel may be calculated for the New Cycle Engine using the following identities:

$$B_{e_{lbm/hr\ fuel}} = \frac{(SFC)(\Delta heat)(m_{charge})(N_{RPM})(60\ min/hr)}{2544\ BTU/hr\text{-}HP} \qquad (62)$$

$$C_p\ fuel \approx (Air/Fuel\ mass\ ratio)(C_p\ combustion\ products) \qquad (63)$$

Substitution of the above identities into equation (61) yields:

(64)

$$Bo^{\#} = \frac{C(SFC)(\Delta heat)(m_{charge})(N_{RPM})(Air/fuel\ mass\ ratio)C_{p_{cp}}}{\varepsilon_f A_{HT} T_f^3}$$

where: $C = 1.3768 \times 10^7$

Calculations of T_f at a known $\bar{T}g$ and ε_f from the $Bo^{\#}$ function requires an iterative process matching an assumed T_f both directly from the generated $\bar{T}g/T_f$ fraction and its coupled $Bo^{\#}$ from Figure 4-7. An increasing ε_f will decrease the $Bo^{\#}$, thus decrease $\bar{T}g/T_f$, resulting in an increased calculated T_f. It is noted, however, that increases in ε_f and T_f are not proportional; over a wide range of $Bo^{\#}$ ($> .6$), $\bar{T}g/T_f$ slope is only slightly positive. At $Bo^{\#}$ greater than 1.2, characteristic of low luminous flames, the value of T_f is essentially independent of $Bo^{\#}$ (thus ε_f) and equal to $\bar{T}g/0.8$.

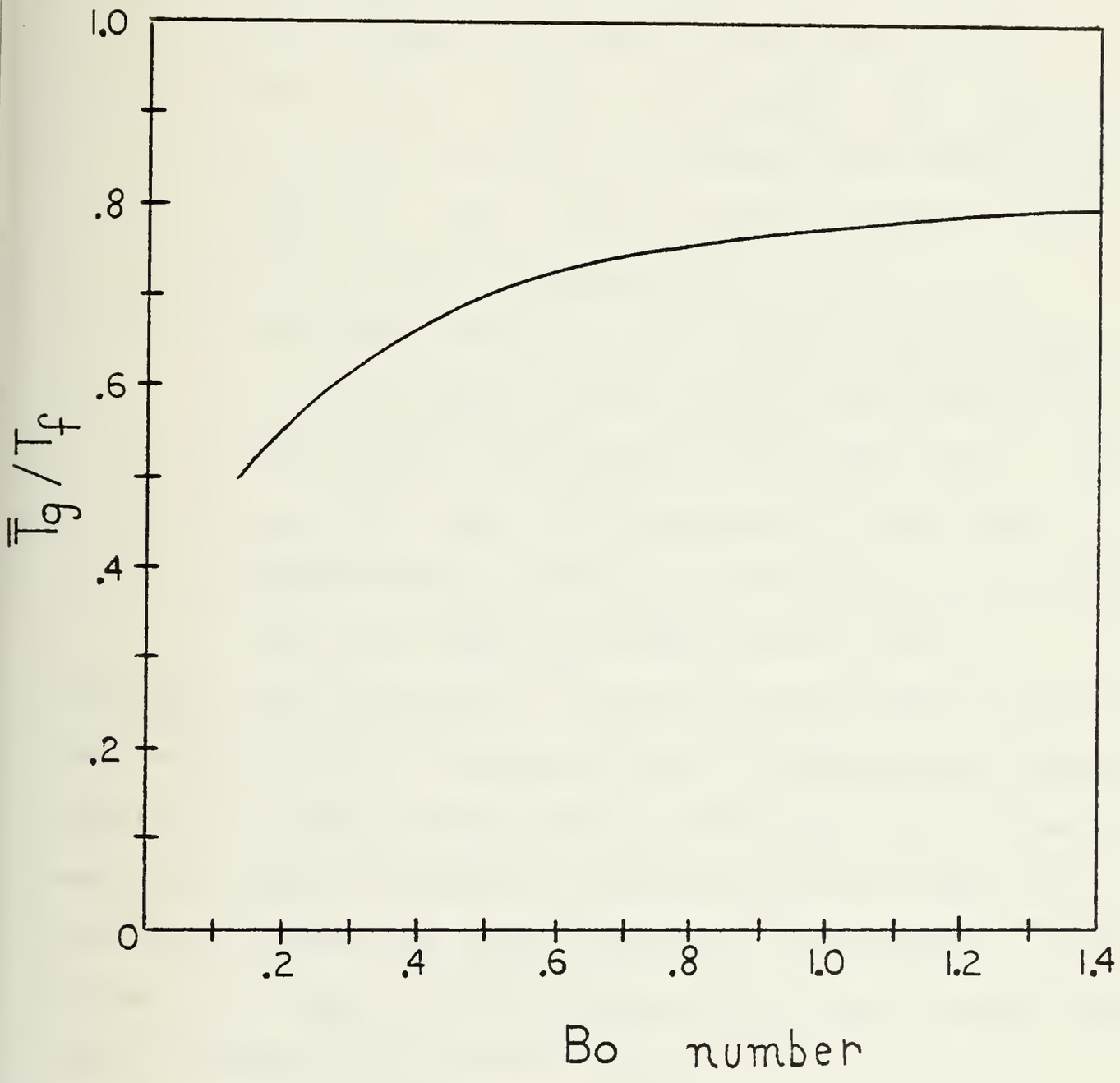

FIGURE 4-7: Variation of $\bar{T}_g/T_f$ in the function of the Bo number [14]

3.8 PREDICTION OF PEAK COMBUSTION ε_a and T_f

For calculation of peak ε_a and T_f in the New Cycle Engine expansion cylinder at full load, the following assumptions are made:

1. The expansion cylinder reflectivity, $\bar{\xi}_w = 0.1$
2. The flame growth encompasses the entire cylinder volume at 20° maximum crank angle from ignition start [crank angle = 65°]; flame growth rate is constant.
3. The flame luminosity, $\mathfrak{L}$, calculation is based on medium speed diesel fuel C/H mass ratio = 6.3
4. The fuel/air mass ratio = .05 (1/20) for Φ = .75
5. $C_{p_{cp}}$ at fuel C/H mass ratio = 6.3 may be approximated by equation (32) as a function of $\bar{T}g$ for C_nH_{2n} fuels (C/H mass ratio = 6.0).

The Sitkei et al method of ε_a calculation was developed on a test engine exhibiting typical high r_c combustion pressure profiles, and TDC ignition start, both conditions not met in New Cycle Engine operation. The peak k_p from Figure 4-4 at the correct excess air factor value will therefore be applied at the crank angle of maximum combustion pressure where flame growth reaches 100% cylinder volume.

Sitkei Method; ε_a peak

$$\theta_{\varepsilon a \text{ peak}} = \underline{65°}$$

$$\text{excess air factor} = (.75)^{-1} = \underline{1.33}$$

$$\text{peak } k_p \text{ at } 1.33 \text{ excess air factor} = \underline{0.63} \quad \text{(see Figure 4-4)}$$

Using equations (47) and (58), plus applying a ε_a correction factor of 2:

θ	P	V	A_{HT}	l_R	k_p	$.3048k_pPl_R$	ε_a	$2\varepsilon_a$
	atm	ft^3	ft^2	ft	$(ft\text{-}atm)^{-1}$			
65°	3.76064	.488331	3.944	.4210	.63	.304	.210	.420

$$\underline{\text{peak } \varepsilon_a = .420} \quad \text{at } \theta = 65°$$

Low Combustion Pressure Power Unit Method, ε_a peak

flame luminosity, $\mathcal{L} = \underline{4.0}$
(see Figure 4-6)

Using Equations (47) and (59):

θ	P	$\bar{T}_g$	V	A	flame growth	$l_R x\%$	Z	ε_a
	atm	°R	ft^3	ft^2	%	ft		
50	4.24684	2259.6	.309053	3.358	25	.0782	.382	.318
55	4.09172	2571.21	.366348	3.545	50	.1757	.455	.366
60	3.92401	2864.13	.426316	3.741	75	.2906	.477	.379
65	3.76064	3136.02	.488331	3.944	100	.4210	.480	.381
70	3.26107	3064.15	.551767	4.152	100	.4518	.447	.360

$$\underline{\text{peak } \varepsilon_a = .381} \quad \text{at } \theta = 65°$$

A repeated calculation for both methods at peak combustion pressure greater than 50 atm, typical for direct injection, high r_c CI engines, results in peak $\varepsilon_a \approx 1.0$, which closely agrees with the expected value ($\approx$0.9).

Boltzmann Number Function Method, peak T_f

The known values required for calculation of the $Bo^{\#}$ at 65° crank angle, peak ε_a of (.420 + .381)/2 = .40 are:

1. $\bar{T}g = 3136.0\ ^{\circ}R$

2. SFC = .284298 lbm fuel/HP-hr

3. Δheat = 500 BTU/lbm charge

4. $m_{charge} = .024537$ lbm

5. $N_{RPM} = 813.3$

6. $C_{p_{cp}} = .247+.243\times10^{-4}(3136.0^{\circ}R) = .3232\ \frac{BTU}{lbm-^{\circ}R}$

7. air/fuel mass ratio = 20

8. $A_{HT} = 3.944\ ft^2$

Substituting the above values into equation (64) yields:

$$Bo^{\#} = \frac{(1.3768\times10^{7})(.28429)(500)(.024537)(818.3)(20)(.3232)}{(3.944)\varepsilon_f T_f^{3}}$$

$$= \frac{6.435\times10^{10}}{\varepsilon_f T_f^{3}}$$

From equation (55), an estimated peak ε_a of 0.40 at an assumed $\bar{\xi}_w = 0.1$ yields a peak ε_f equal to 0.426. The predicted peak T_f may therefore be calculated from iteration using Figure 4-7 at $Bo^{\#}$ equal to:

$$Bo^{\#} = \frac{6.435\times10^{10}}{.426T_f^{3}} = \frac{1.511\times10^{11}}{T_f^{3}}$$

Assuming a value of $T_f = \bar{T}g/0.8 = 3920^{\circ}R$, the calculated $Bo^{\#}$ equal to 2.51. This $Bo^{\#}$ is greater than 1.2, therefore the estimated peak T_f equals 3920°R. Rounding off for first approximation:

$$\underline{\text{peak } T_f = 4000^{\circ}R}$$

To check the accuracy of this procedure, a peak ε_f value of 1.0 is assumed commensurate with observed peak ε_a in direct injection, high r_c CI engines:

$$Bo^{\#} = \frac{6.435 \times 10^{10}}{(1.0)T_f^{3}} = \frac{6.435 \times 10^{10}}{T_f^{3}}$$

From Figure 4-5, the observed peak T_f is typically equal to 4200°R; $\bar{T}g/T_f$ now equals 0.75. Substituting 4200°R into $Bo^{\#} = 6.435 \times 10^{10}/T_f^{3}$ yields a value of 0.87 which, entering Figure 4-7, extrapolates to $\bar{T}g/T_f = 0.76$. The iteration essentially matches, indicating that a peak ε_a and peak T_f equal to 1.0 and 4200°R respectively, are in fact reasonable values for direct injection, high r_c CI engines.

4. CALCULATION OF ORDER OF MAGNITUDE REDUCTION IN COMBUSTION RADIANT HEAT FLUX

Woschni did not separately measure radiant heat flux in his engine testing; for ease of calculation he simply absorbed the radiant component into the forced convection heat transfer model by use of time averaged, "curve fitting" multiplicity coefficients. Woschni in fact believed that [9, pp. 3074 - 3075]:

> "the total radiation amounts to no more than 20% of the total combustion term...In steady flames there are usually large combustion chambers with great volumes of flames, and because of the small velocities there are small convective heat transfer rates only, so that in these cases radiation is responsible for an appreciable amount of the total heat. Because of the high velocity and density of gas, the convective heat transfer coefficients in internal combustion engines are about ten times higher, so that despite the higher temperatures the radiation plays an appreciably smaller part."

While the thrust of the statement is correct, Woschni unfortunately underestimated Q_R, basing cursory radiant heat transfer calculations on the assumption of $\varepsilon_a = 0.6$ from steady state flame observations and employing for the unknown radiant temperature, $\bar{T}g$, vice T_f.

For the purpose of this calculation, establishing Woshni peak ε_a and T_f values of 1.0 and 4200°R better conforms to published data on CI engine testing of similar design, direct injection, high r_c characteristics. It is noted that actual observed peak ε_a values are typically equal to 0.9 vice 1.0. To maintain continuity with ε_a prediction methods used in section 3.8, however, a value of unity is

assumed as predicted for high peak pressure conditions. Without knowledge of the radiant component of q_W and q_{NCE} as a function of crank angle, it is not practical to attempt calculation of a mean order of magnitude reduction ratio, $\overline{q_W/q_{NCE}}$, over the effective 90° crank angle domain where luminous radiant heat transfer can be significant ($\varepsilon_a \triangleq 0.1$) in high r_c, medium speed CI engines. Fortunately, in this case it is not required. Making the reasonable assumption of equivalent ε_a, T_f decay rates, flame emissivity in the New Cycle Engine expansion cylinder should certainly decay below 0.1 at advancing crank angles from ignition start prior to +90°. Thus, peak q_W/q_{NCE} should be a <u>minimum</u>, conservative estimation of the mean. Therefore, from equation (56):

$$\underline{\text{radiation}}\quad \frac{\bar{q}_W}{q_{NCE}} \propto \frac{q_W}{q_{NCE}}_{peak} \propto \frac{\varepsilon_a(T_f^4-\bar{T}w^4)_W}{\varepsilon_a(T_f^4-\bar{T}w^4)_{NCE}}_{peak}$$

$$\bar{T}_w = 900°R$$

Substituting in the respective ε_a and T_f values previously determined:

$$\text{minimum}\ \frac{\bar{q}_W}{q_{NCE}} = \frac{1.0(4200^4-900^4)}{0.4(4000^4-900^4)} = 3.047 \text{ approx.}$$

CHAPTER FIVE

CALCULATION OF CORRECTED HEAT TRANSFER LOSS/HEAT RELEASE PER CYCLE, $\mathfrak{R}^*$

Total heat transfer loss, Q_T, for a natural aspirating, four stroke CI engine includes heat transfer during the induction and compression strokes which do not exist in the two stroke New Cycle Engine expansion cylinder cycle. In the induction stroke, the heat transfer driving potential, $\bar{T}g-\bar{T}w$, is negative; induction charge heating is boosted by residual gas mixing. In the compression stroke, adiabatic compression may boost $\bar{T}g$ to greater than 1500°R. From Figure 2-1, it is observed that a significant positive $\bar{T}g-\bar{T}w$ occurs only in the last 30° of the compression stroke. The order of magnitude of this positive driving potential compared to that observed in the combustion-expansion and exhaust strokes is still quite small. It may therefore be assumed that the induction and compression stroke contribution to Q_T for a natural aspirating, four stroke, high r_c CI engine is not significant. A direct coupling of observed Q_R/Q_T ratios may then be applied to the New Cycle Engine expansion cylinder.

From Chapters 2, 3, and 4, the following principal values have been determined:

1. $\mathfrak{R}_T$ uncorrected = 19.761%; Woschni correlations
2. Q_R/Q_T Woschni engine $\equiv \Psi$; $.2 \triangleq \Psi \triangleq .3$

3. Forced convection $\overline{q_W/q_{NCE}} = 6.087$

4. Radiation $\overline{q_W/q_{NCE}} = 3.047$ minimum

$\mathcal{R}_T$ must be corrected for the failure of Woschni's correlation, based solely on a theoretical forced convective heat transfer model, to properly scale down luminous radiation heat transfer to low r_c operating conditions.

Correction to $\mathcal{R}_T = \mathcal{R}_{FC} + \mathcal{R}_R$

At high r_c operation:

$$\frac{Q_R}{Q_T} = \frac{Q_R/(\Delta heat)(m_{charge})}{(Q_R + Q_{FC})/(\Delta heat)(m_{charge})} = \frac{\mathcal{R}_R}{\mathcal{R}_R + \mathcal{R}_{FC}} = \Psi$$

$$\mathcal{R}_R = \Psi\mathcal{R}_R + \Psi\mathcal{R}_{FC}$$

$$\mathcal{R}_R(1-\Psi) = \Psi\mathcal{R}_{FC}$$

$$\mathcal{R}_R = \frac{\Psi}{1-\Psi}\,\mathcal{R}_{FC} \qquad (65)$$

Substituting into equation (65) the known order of magnitude reduction ratios for low r_c operating conditions and establishing equality:

At low r_c operation:

$$3.047\ \mathcal{R}_R^* = \frac{\Psi}{1-\Psi}\ 6.087\ \mathcal{R}_{FC}^*$$

$$\mathcal{R}_{R\ maximum}^* = 2.00\ \frac{\Psi}{1-\Psi}\ \mathcal{R}_{FC}^* \qquad (66)$$

As Woschni's correlation properly scales down forced convection heat transfer only, $\mathcal{R}_{FC}^* = (1 - \Psi)\mathcal{R}_T$. Therefore a conservative, first approximation prediction of corrected total heat transfer loss/heat release per cycle, $\mathcal{R}_T^*$, for $.2 \leq \Psi \leq .3$ is :

1. Forced convection heat transfer loss, $\mathfrak{R}_{FC}^{*}$

$$\mathfrak{R}_{FC}^{*} = (1-\Psi)\mathfrak{R}_{T} = (1-\Psi)19.761\%$$

$$\underline{13.837\% \leq \mathfrak{R}_{FC}^{*} \leq 15.809\%}$$

2. Radiant heat transfer loss, $\mathfrak{R}_{R}^{*}$

$$\mathfrak{R}_{R}^{*} = 2.00\left(\frac{\Psi}{1-\Psi}\right)\mathfrak{R}_{FC}^{*} = 2.00\left(\frac{\Psi}{1-\Psi}\right)(1-\Psi)\mathfrak{R}_{T}$$

$$= 2.00\ \Psi\ \mathfrak{R}_{T}$$

$$= 2.00\ \Psi\ 19.761\%$$

$$\underline{7.904\% \leq \mathfrak{R}_{R}^{*} \leq 11.857\%}_{\text{maximum}}$$

3. Total heat transfer loss, $\mathfrak{R}_{T}^{*}$

$$\mathfrak{R}_{T}^{*} = \mathfrak{R}_{R}^{*} + \mathfrak{R}_{FC}^{*} = 2.00\Psi\mathfrak{R}_{T} + (1-\Psi)\mathfrak{R}_{T}$$

$$= (2.00\Psi+1-\Psi)\mathfrak{R}_{T}$$

$$= (1+\Psi)\mathfrak{R}_{T}$$

$$= (1+\Psi)\ 19.761\%$$

$$\underline{23.713\% \leq \mathfrak{R}_{T}^{*} \leq 25.689\%}_{\text{maximum}}$$

CHAPTER SIX

CONCLUSIONS AND RECOMMENDATIONS FOR FUTURE STUDY

A semi-empirical correlation for mean instantaneous heat transfer coefficient, developed by Woschni on conventional four stroke, direct injection, quiescent CI engines, was modified to predict heat transfer loss in a computer-generated preliminary design engine cycle. The engine divides the four stroke functions between a compression cylinder and an expansion cylinder interconnected by a static regenerative heat exchanger. Due to regenerator boost heating of the air charge, required compression ratios in the New Cycle Engine expansion cylinder will be significantly reduced, and increased thermal efficiency achieved. To verify applicability of Woschni's correlation to expansion cylinder heat transfer, points in the cycle were examined comparing Woschni's correlation to fully developed, turbulent flow, forced convection relationships for flat plate and pipe flow. The mean instantaneous gas velocity was estimated from the construction of the charge impulse transient existing into the expansion cylinder from the regenerator port. An order of magnitude reduction in forced convection and luminous radiant heat flux was calculated to investigate the ability of Woschni's correlation to scale down correctly total heat transfer to low compression ratio operation.

It was found that the impulse velocity transient was sufficiently suppressed to approximate quiescent conditions. It was found that laws of similarity incorporated into Woschni's correlation appear to allow uncorrected application at low compression ratio operation for forced convection heat transfer only. The order of magnitude reduction in combustion-expansion stroke forced convection heat flux was found to be as much as twice the order of magnitude reduction in radiant heat flux. A correction was proposed for the application of Woschni's correlation to achieve a conservative prediction of heat transfer loss in the New Cycle engine expansion cylinder cycle:

$$Q_{T_{corrected}} = 1.25\ Q_{T_{uncorrected}} \qquad (67)$$

where: $Q_{T_{uncorrected}} = \int \dot{Q}\ d\theta$

$$\dot{Q} = \bar{h}_e\ A_{HT}\ (\bar{T}g - \bar{T}w)$$

$$\bar{h}_e = 15.480\ P^{.8}\ [C_1 \bar{S}p]^{.8}\ B^{-.2}\ \bar{T}g^{-.53}$$

C_1 = 6.18 exhaust stroke
2.28 combustion-expansion stroke

This study investigated heat transfer in engine operating conditions significantly below the range for which published correlations exist. Theoretical work and actual measurement of an engine prototype remain to be completed to prove the validity of significant extrapolation of reciprocating engine heat transfer correlations. This study points out three specific areas requiring future study concerning reciprocating engine heat transfer prediction:

1. Quantitative prediction of flow pattern magnitude and distribution as a function of crank angle and location.
2. Quantitative prediction of soot concentration, apparent flame emissivity, and radiant temperature as a function of operational variables in low pressure diffusion flame combustion.
3. Quantitative effect of appreciable fuel injection and ignition delay in the expansion stroke of low compression ratio reciprocating engines on incandescent particle concentration and luminous flame radiation.

REFERENCES

(1) Carmichael, A. Douglas, Professor of Power Engineering, Massachusetts Institute of Technology, September 1983.

(2) Rohsenhow, W. and Choi, H., Heat, Mass, and Momentum Transfer, Prentice-Hall, Inc., Englewood Cliffs, N.J., 1961.

(3) Annand, W., "Heat Transfer from Flames in Internal Combustion Engines", Heat Transfer in Flames, N. Afgran and J. Beer, eds., Scripta Book Company, Washington D.C., 1974, Chapter 24, pp. 377-390.

(4) Hohenberg, G., "Advanced Approaches for Heat Transfer Calculation", S.A.E. Transactions, Vol. 88, 1979, Paper 790825, pp. 2788-2806.

(5) LeFeuvre, T., Myers, P., and Uyehara, O. "Experimental Instantaneous Heat Fluxes in a Diesel Engine and Their Correlation", S.A.E. Transactions, Vol. 78, 1969, Paper 690464, pp. 1717-1739.

(6) Annand, W., "Heat Transfer in the Cylinders of Reciprocating Internal Combustion Engines", Proc. Instn. Mech. Engrs., Vol. 177, 1963, pp. 973-990.

(7) Mansuri, S. and Heywood, J., "Correlations for the Viscosity and Prandtl Number of Hydrocarbon-Air Combustion Products", Combustion Science and Technology, Vol. 23, 1980, pp. 251-256.

(8) Oguri, T. and Inaba, S., "Radiant Heat Transfer in Diesel Engines", S.A.E. Transactions, Vol. 81, 1972, Paper 720023, pp. 127-143.

(9) Woschni, G., "A Universally Applicable Equation for the Instantaneous Heat Transfer Coefficient in the Internal Combustion Engine", S.A.E. Transactions, Vol. 76, 1967, Paper 670931, pp. 3065-3084.

(10) Dent, J. and Sulaiman, S., "Convective and Radiative Heat Transfer in a High Swirl Direct Injection Diesel Engine", S.A.E. Transactions, Vol. 86, 1977, Paper 770407, pp. 1758-1783.

(11) Alcock, J. and Scott, W., "Some More Light on Diesel Combustion", Proc. Instn. Mech. Engrs., Automotive Division Proceedings, 1962-1963, pp. 179-200.

(12) Fitzgeorge, D., and Allison, J., "Air Swirl in a Road Vehicle Diesel Engine", Proc. Instn. Mech. Engrs., Automotive Division Proceedings, 1962-1963, pp. 151-178.

(13) Heinein, N., "Instantaneous Heat Transfer Rates and Coefficients Between the Gas and Combustion Chamber of a Diesel Engine", S.A.E. Transaction, Vol. 74, 1965, Paper 650096, pp. 1-11.

(14) Sitkei, G., Heat Transfer and Thermal Loading in Internal Combustion Engines, P. Szoke transl., Akadémiai Kiadó, Budapest, 1974.

(15) Sitkei, G. and Ramanaiah, G., "A Rational Approach for Calculation of Heat Transfer in Diesel Engines", S.A.E. Transactions, Vol. 81, 1972, Paper 720027, pp. 165-174.

(16) Flynn, P., Mizusawa, M., Uyehara, O. and Myers, P., "An Experimental Determination of the Instantaneous Potential Radiant Heat Transfer Within an Operating Diesel Engine", S.A.E. Transaction, Vol. 81, 1972, Paper 720022, pp. 95-126.

(17) Chapman, M., Friedman, M. and Aghan, A., "A Time-Dependent Spatial Model for Radiant Heat Transfer in Diesel Engines", S.A.E. Transaction, Vol. 92, 1983, Paper 831725, pp. 13-20.

(18) Khan, I. and Greeves, G., "A Method for Calculating the Formation and Combustion of Soot in Diesel Engines", N. Afgran and J. Beer, eds., Scripta Book Company, Washington D.C., Chapter 25, pp. 391-403.

(19) Kretschmer, D. and Odgers, J., "A Simple Method for the Prediction of Wall Temperatures in Gas Turbines", ASME, 1978, Paper 78-GT-90, pp. 1-7.

APPENDIX A

The purpose of this appendix is to present preliminary design parameters and the computer-generated thermodynamic firing cycle for the New Cycle Engine expansion cylinder on which the heat transfer calculations are based [1]:

Preliminary Design Parameters; expansion cylinder

1. Mean piston speed, $\bar{S}_p$ = 2000 ft/min (33.33 ft/sec)
2. Square configuration; stroke = bore diameter (L=B)
3. Neglect clearance volume; Vc = 0
4. Neglect cylinder sleeve clearance
5. Regenerator port exit cross-section area, A_p = 0.80 ft^3 (1/3rd cylinder circumference x .75 inch depth)
6. Compression cylinder supercharge pressure ratio=1; natural aspirating
7. Quiescent fuel injection at nominal 25° crank angle
8. Ignition start at nominal 45° crank angle
9. Specific heat release per cycle, Δheat = 500 BTU/lbm charge.
10. Specific fuel consumption, SFC = .284298 lbm/HP-hr
11. Fuel base = nominal C_nH_{2n} medium speed diesel fuel
12. Full load equivalence ratio, Φ = .75
13. Full load air/fuel mass ratio = 20
14. Mean heat transfer surface wall temperature, $\bar{T}w$ = 900°R
15. Specific gas constant for air charge and combustion products, R = 53.90 lbf-ft/lbm-°R
16. Air charge Prandtl number, Pr = .70

TABLE A-1

New Cycle Engine expansion cylinder computer-generated thermodynamic firing cycle model as a function of crank angle; 5° increments [1]

crank angle θ°	Pressure P, atm	mean gas temp. $\bar{T}g$, °R	Volume V, ft^3
EXPANSION-INDUCTION CONDITIONS			
5	2.49823	2149.04	3.4067E-03
10	3.1201	2159.25	.0135883
15	3.91693	2195.73	.0304243
20	4.83479	2225.26	.0537145
25	5.67408	2229.71	.0831858
30	6.10171	2194.29	.118493
35	5.88219	2116.61	.159226
40	5.12078	2010.57	.204916
45	4.14883	1896.6	.255045
EXPANSION-COMBUSTION CONDITIONS			
50	4.24684	2251.6	.309053
55	4.09172	2571.21	.366348
60	3.92401	2864.13	.426316
65	3.76064	3136.02	.488331
70	3.26107	3064.15	.551767
75	2.88976	2998.73	.616005
80	2.58662	2939.11	.680446
85	2.33694	2884.75	.744518
90	2.12966	2835.18	.887682
95	1.95638	2789.98	.869441
100	1.81064	2748.78	.929342
105	1.68741	2711.25	.98698
110	1.58277	2677.09	1.042
115	1.49361	2646.03	1.09408
120	1.41745	2617.83	1.14298
125	1.35232	2592.29	1.18847
130	1.29661	2569.22	1.23038
135	1.24904	2548.44	1.26857
140	1.20857	2529.82	1.30291
145	1.17433	2513.21	1.33334
150	1.14565	2498.51	1.3598
155	1.12197	2485.62	1.38223
160	1.10286	2474.46	1.40061
165	1.08796	2464.96	1.41492
170	1.07702	2457.07	1.42515
175	1.06986	2450.74	1.43129
BDC	1.06636	2445.96	1.43333

TABLE A-1 (CONT'D)

θ°	P, atm	$\overline{T}g$, °R	V, ft^3
EXHAUST CONDITIONS			
BDC	1.05	2439.06	1.43333
185	1.05	2434.63	1.43129
190	1.05	2430.7	1.42515
195	1.05	2426.81	1.41492
200	1.05	2422.95	1.40061
205	1.05	2419.13	1.38223
210	1.05	2415.36	1.3598
215	1.05	2411.64	1.33335
220	1.05	2407.99	1.30292
225	1.05	2404.41	1.26858
230	1.05	2400.9	1.23039
235	1.05	2397.47	1.18849
240	1.05	2394.14	1.143
245	1.05	2390.89	1.0941
250	1.05	2387.75	1.04201
255	1.05	2384.71	.985995
260	1.05	2381.77	.929358
265	1.05	2378.95	.863458
270	1.05	2376.24	.8077
275	1.05	2373.65	.744536
280	1.05	2371.18	.680464
285	1.05	2368.82	.616023
290	1.05	2366.58	.551785
300	1.05	2364.46	.488348
305	1.05	2362.44	.426333
310	1.05	2360.54	.366364
315	1.05	2358.73	.309069
320	1.05	2357.03	.255059
325	1.05	2355.41	.204929
330	1.05	2353.88	.159238
335	1.05	2352.41	.118504
340	1.05	2351.01	.083195
345	1.05	2349.67	.053722
350	1.05	2348.36	.0304295
355	1.05	2347.09	.0135921
TDC	1.05	2345.83	3.4083E-03
		2344.58	0

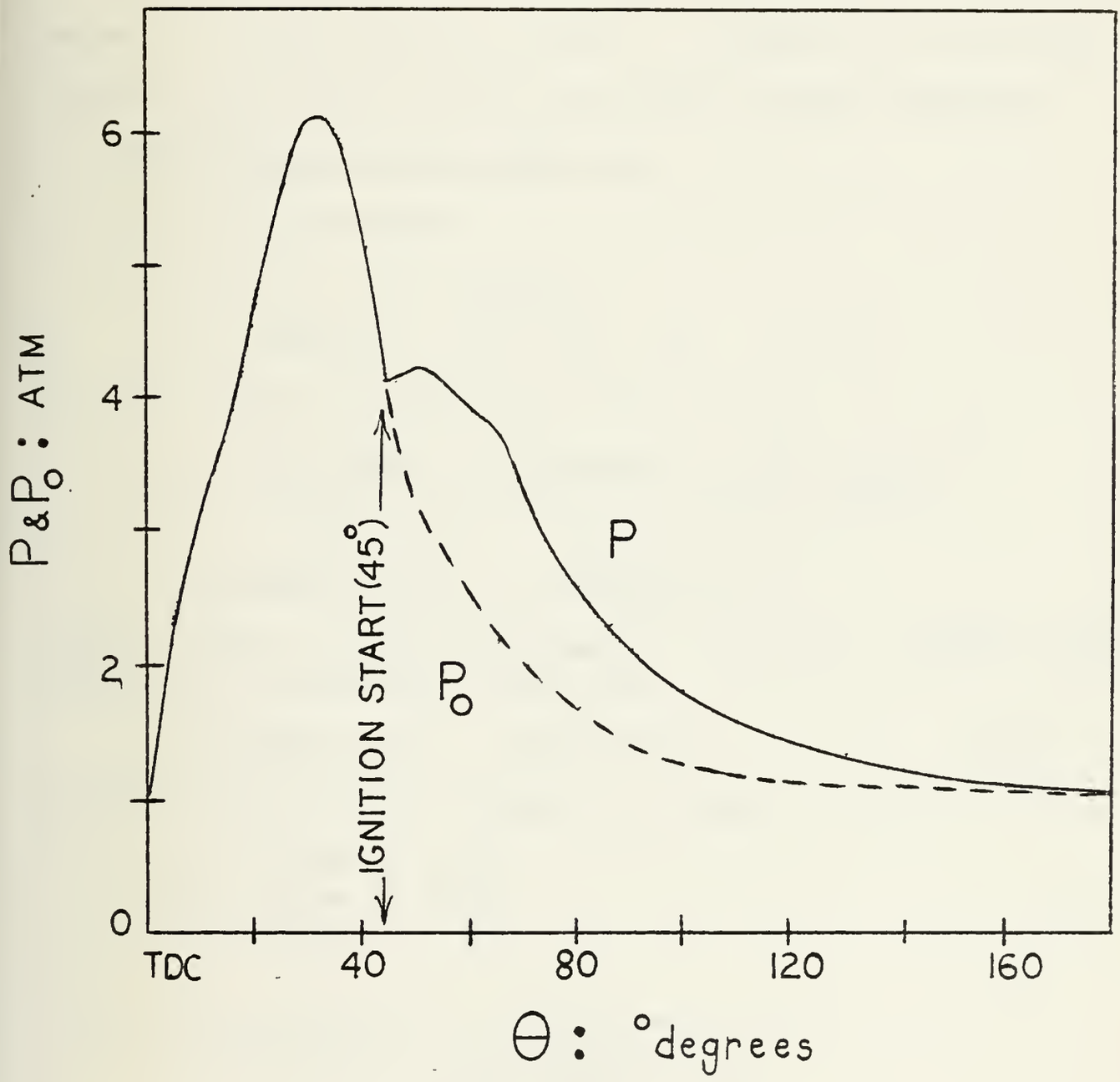

FIGURE A-1: Generation of expansion cylinder firing cycle motoring P_o

APPENDIX B

The purpose of this Appendix is to present the derivation of several geometric relations for a simple geometry reciprocating cylinder. Figure B-1 illustrates a standard cylinder with defined piston linkage symbology.

1. Instantaneous piston speed, Sp

by the law of cosines:

$$l_r^2 = s^2 + a^2 + 2as\cos\theta$$

$$s^2 - (2a\cos\theta)s + (a^2 - l_r^2) = 0$$

by the quadratic formula, solving for s:

$$s = \frac{-(-2a\cos\theta) \pm [(2a\cos\theta)^2 - 4(a^2 - l_r^2)]^{1/2}}{2}$$

$$s = a\cos\theta \pm [l_r^2 + a^2(\cos^2\theta - 1)]^{1/2}$$

substituting in the trigonometric identity, $\cos^2\theta - 1 = \sin^2\theta$, and taking the positive real root:

$$s = a\cos\theta + [l_r^2 - a^2\sin^2\theta]^{1/2} \qquad (B-1)$$

differentiating s with respect to time, t:

$$Sp = \frac{ds}{d\theta}\frac{d\theta}{dt} = \dot{\theta}\frac{ds}{d\theta}$$

$$Sp = \dot{\theta}\left[-a\sin\theta - \frac{a^2\sin\theta\cos\theta}{(l_r^2 - a^2\sin^2\theta)^{1/2}}\right]$$

substituting in the crank ratio identity, $R_c = l_r/a$, and simplifying:

$$Sp = -a\dot{\theta}\sin\theta\left[1 + \frac{\cos\theta}{(R_c^2 - \sin^2\theta)^{1/2}}\right]$$

substituting in the $\dot{\theta}$ identity, $\dot{\theta} = 2\pi N_{RPM}/60$:

$$Sp = \frac{-a2\pi N_{RPM}\sin\theta}{60}\left[\,1 + \frac{\cos\theta}{(R_c^{\,2}-\sin^2\theta)^{1/2}}\,\right] \qquad (B\text{-}2)$$

2. Mean Piston Speed, $\bar{S}p$:

$$\bar{S}p = \frac{1}{\pi}\int_0^{\pi} Sp\ d\theta$$

$$= \frac{1}{\pi}\int_0^{\pi} \frac{-a2\pi N_{RPM}\sin\theta}{60}\left[1+\frac{\cos\theta}{(R_c^{\,2}-\sin^2\theta)^{1/2}}\,\right] d\theta$$

$$= \frac{-2aN_{RPM}}{60}\left[\int_0^{\pi}\sin\theta\ d\theta + \int_0^{\pi}\frac{\sin\theta\cos\theta}{(R_c^{\,2}-\sin^2\theta)^{1/2}}d\theta\,\right]$$

$$= \frac{-2aN_{RPM}}{60}\left[\,2 + \int_0^{\pi}\frac{\sin\theta\cos\theta}{(R_c^{\,2}-\sin^2\theta)^{1/2}}\,d\theta\,\right]$$

Let $u = \cos\theta$ and substitute into the integrand the equivalent identities:

$$du = -\sin\theta$$

$$\sin^2\theta = 1-\cos\theta = 1-u^2$$

$$\cos(\pi) = -1$$

$$\cos(0) = 1$$

$$\bar{S}p = \frac{-2aN_{RPM}}{60}\left[\,2 + \int_{+1}^{-1}\frac{-u}{(R_c^{\,2}-1+u^2)^{1/2}}\,du\,\right]$$

$$= \frac{-2aN_{RPM}}{60}\left[\,2 + \int_{-1}^{+1}\frac{u}{(R_c^{\,2}-1+u^2)^{1/2}}\,du\,\right]$$

$$= \frac{-2aN_{RPM}}{60}\left(\,2 + \left[R_c^{\,2}-1+u^2\right]^{1/2}\Big|_{-1}^{+1}\right)$$

$$\bar{S}p = \frac{-2aN_{RPM}}{60} \quad (2+0)$$

$$\bar{S}p = \frac{-4aN_{RPM}}{60}$$

Substituting in the crank radius identity, a = L/2:

$$\bar{S}p = \frac{2LN_{RPM}}{60} \quad (B-3)$$

3. Instantaneous Cylinder Volume, V:

Neglecting clearance volume, V_c, and sleeve clearance:

$$V = \frac{\pi B^2}{4} L_\theta \quad (B-4)$$

4. Instantaneous Heat Transfer Area, A_{HT}:

Neglecting clearance volume, V_c, and sleeve clearance:

$$A_{HT} = 2(\frac{\pi B^2}{4}) + \pi B L_\theta \quad (B-5)$$

where: $L_\theta = l_r + a - s$
s from equation (B-1)

5. Calculation of New Cycle Engine Expansion Cylinder Preliminary Design Parameters:

B, L, l, a, R, N_{RPM}, max Sp

From Appendix A, the following preliminary design conditions are known:

a. Clearance volume, $V_c = 0$: $L_\theta = l_r + a - s$

b. Sleeve clearance = 0 : B = bore and piston diameter

c. Square configuration : B = L

d. $\bar{S}p = 33.\overline{33}$ ft/sec

e. $V_{BDC} = 1.43333$ ft^3

f. $V_{90°} = 0.80770$ ft^3

At V_{BDC}, $L_\theta = L = B$:

$$V_{BDC} = 1.43333 \text{ ft}^3 = \frac{\pi B^2}{4} L_\theta = \frac{\pi B^3}{4} \qquad \text{(B-4)}$$

$$B = L = \left[\frac{4(1.43333)}{\pi} \right]^{1/3}$$

$$\underline{B = L = 1.22204 \text{ ft}}$$

From the crank radius identity, $a = L/2$:

$$\underline{a = 0.61102 \text{ ft}}$$

From equations (B-1), (B-4), and the geometric relationship, $L_\theta = l_r + a - s$ at a given crank angle θ:

$$\frac{4V}{\pi B^2} = l_r + a - [a\cos\theta + (l_r^2 - a^2\sin^2\theta)^{1/2}]$$

which at known V, B, and a values at $\theta = 90°$ simplifies to:

$$\frac{4(.8077)}{\pi(1.22204)^2} = l_r + .61102 - [.61102\cos 90° + (l_r^2 - .61102^2 \sin^2 90°)^{1/2}]$$

$$l_r - .077615 = (l_r^2 - .373346)^{1/2}$$

$$l_r^2 - .155231 l_r + .006024 = l_r^2 - .373346$$

$$\underline{l_r = 2.4440 \text{ ft}}$$

From the crank ratio identity, $R_c = l_r/a$:

$$\underline{R_c = 4.0}$$

From equation (B-3), $N_{RPM} = 60\ \bar{S}p/2L$:

$$N_{RPM} = \frac{60(30.\overline{33})}{2(1.22204)}$$

$$\underline{N_{RPM} = 818.3}$$

From equation (B-2), recognizing that maximum Sp occurs at $\theta = 90°, 270°$:

$$Sp_{max} = \frac{a2\pi N_{RPM} \sin 90°}{60} \left[1 + \frac{\cos 90°}{(R_c^2 - \sin^2 90°)^{1/2}} \right]$$

$$Sp_{max} = \frac{a 2\pi N_{RPM}}{60}$$

$$= \frac{(.61102)(2\pi)(818.3)}{60}$$

$$\underline{Sp_{max} = 52.36 \text{ ft/sec}}$$

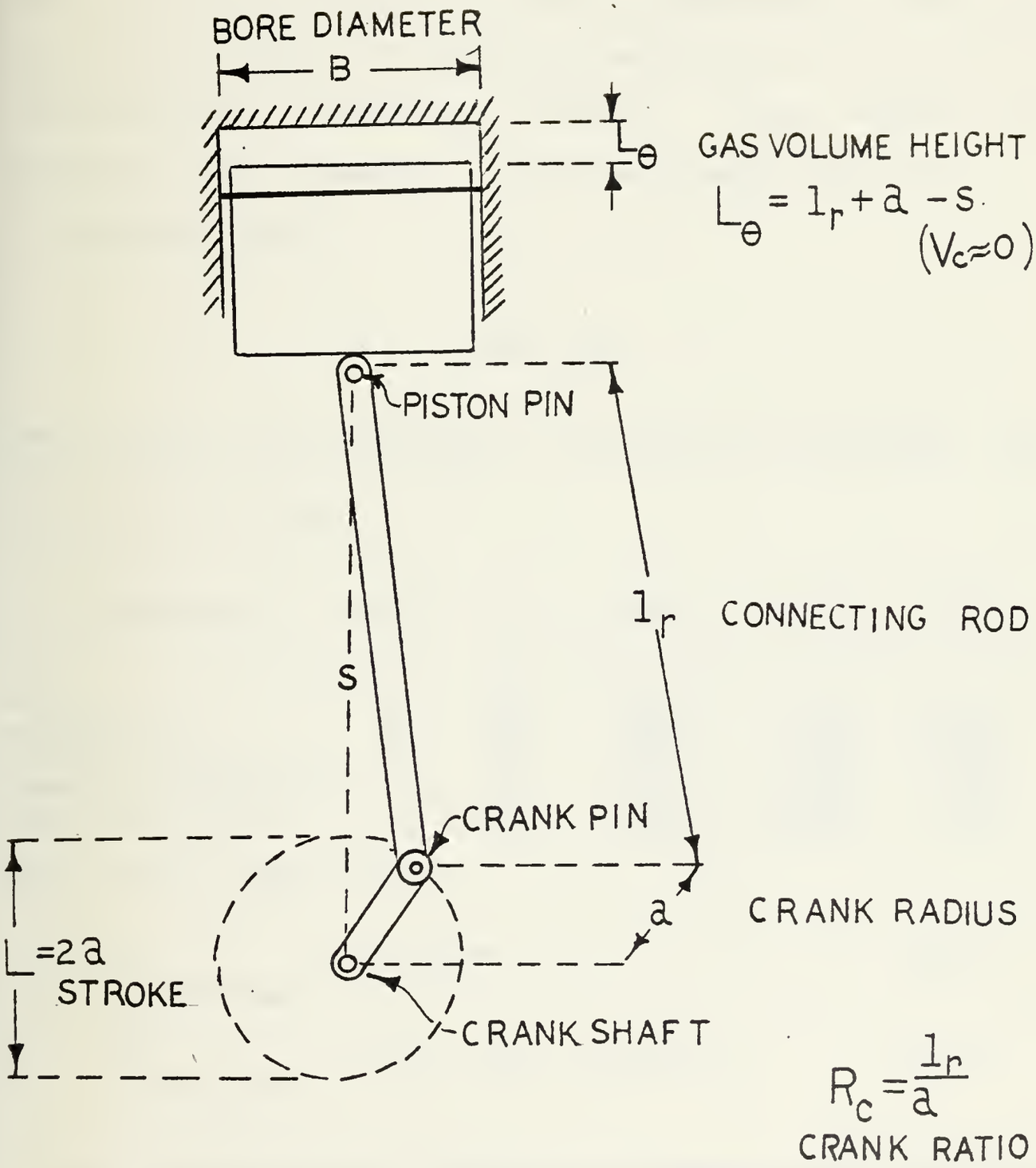

FIGURE B-1: Standard reciprocating cylinder and piston linkage geometry

APPENDIX C

The purpose of this appendix is to present formulas for calculation of essential thermal properties of principle gases as a function of mean gas temperature, $\bar{T}g$, and lean hydrocarbon-air combustion products, C_nH_{2n} fuels, as a function of $\bar{T}g$, pressure, P, and equivalence ratio, Φ.

1. Principle gases

TABLE C-1

Coefficients for calculation of C_p and μ of principle gases as a function of $\bar{T}g$(°R) [6]

Valid for Tg > 450°R

Substance	AMW	Y_0	10^4Y_1	10^8Y_2	$10^7\mu_o$
air	29	.224	.2617	.00	2.163
nitrogen N_2	28	.233	.2478	-.0012	2.101
carbon monoxide CO	28	.229	.3306	-.2160	2.053
carbon dioxide CO_2	44	.141	1.3128	-2.4867	1.704
water vapor H_2O	18	.479	-.4483	4.8951	1.499

AMW = Atomic Mass Weight

$$\mu_{\text{lbm/ft-sec}} = \mu_o \bar{T}g^{.645} \qquad \text{(C-1)}$$

$$C_{p_{\text{BTU/lbm-°R}}} = Y_0 + Y_1\bar{T}g + Y_2(\bar{T}g)^2 \qquad \text{(C-2)}$$

2. Lean Hydrocarbon-Air Combustion products; C_nH_{2n} fuels [7]

Valid for 900°R ≤ $\bar{T}g$ ≤ 7200°R and Φ ≤ 1.0:

$$\mu_{\text{lbm/ft-sec}} = \frac{1.470\times10^{-7}(\bar{T}g)^{.7}}{1+.027\Phi} \qquad \text{(C-3)}$$

$$Pr = 0.05 + 4.2(\gamma-1) - 6.7(\gamma-1)^2 \qquad (C-4)$$

$\gamma(\bar{T}g) \equiv$ Figure C-2

Valid for 900°R $\leq \bar{T}g \leq$ 3600°R, P = 1 atm, and Φ = .75 (see Figure C-2):

$$C_{p_{BTU/lbm-°R}} = .247 + .243 \times 10^{-4} \bar{T}g \qquad (C-5)$$

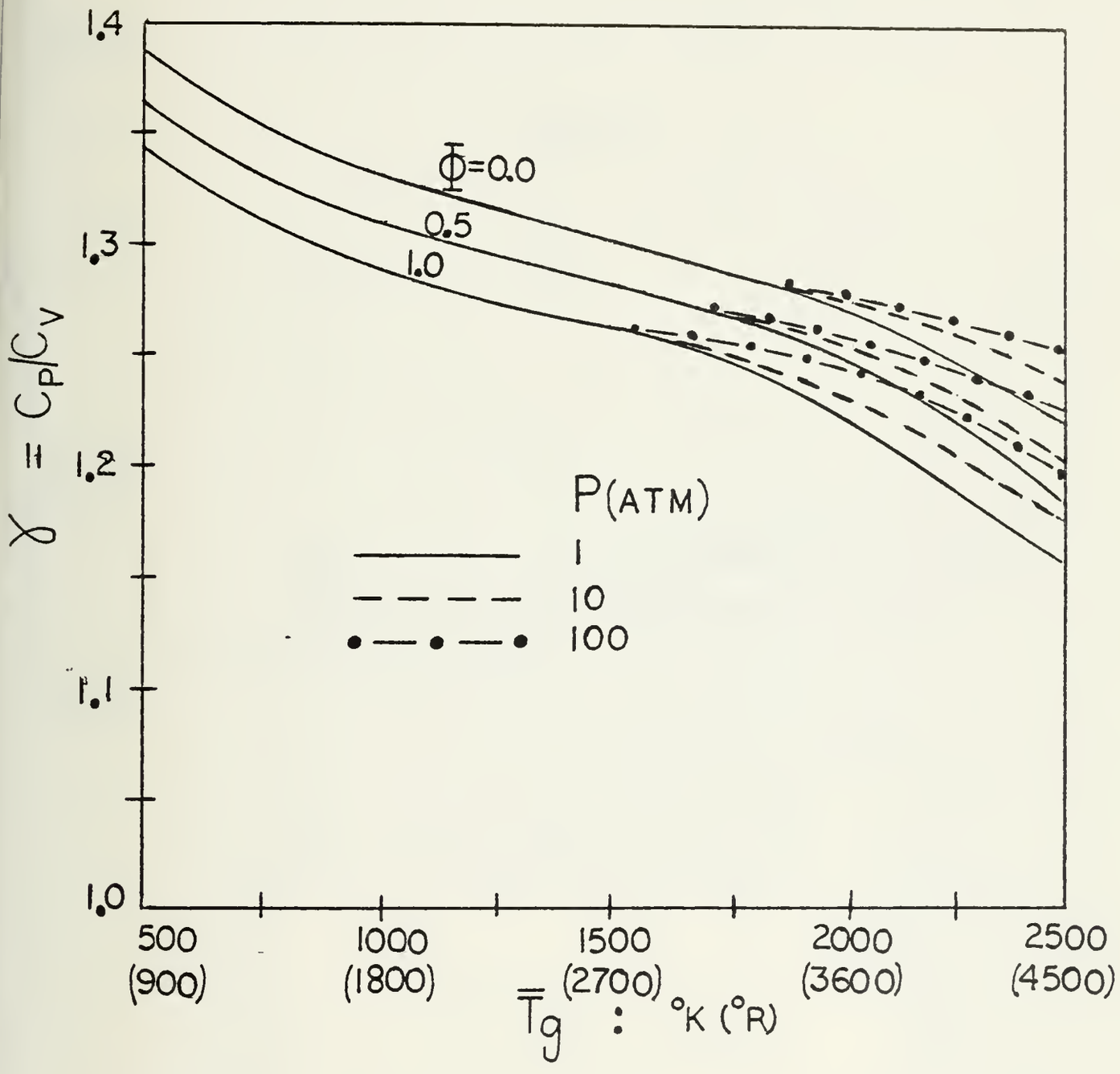

FIGURE C-1: Ratio of specific heats, γ, of lean hydrocarbon-air combustion products as a function of P, $\bar{T}g$, and Φ; fuel C_nH_{2n} [7]

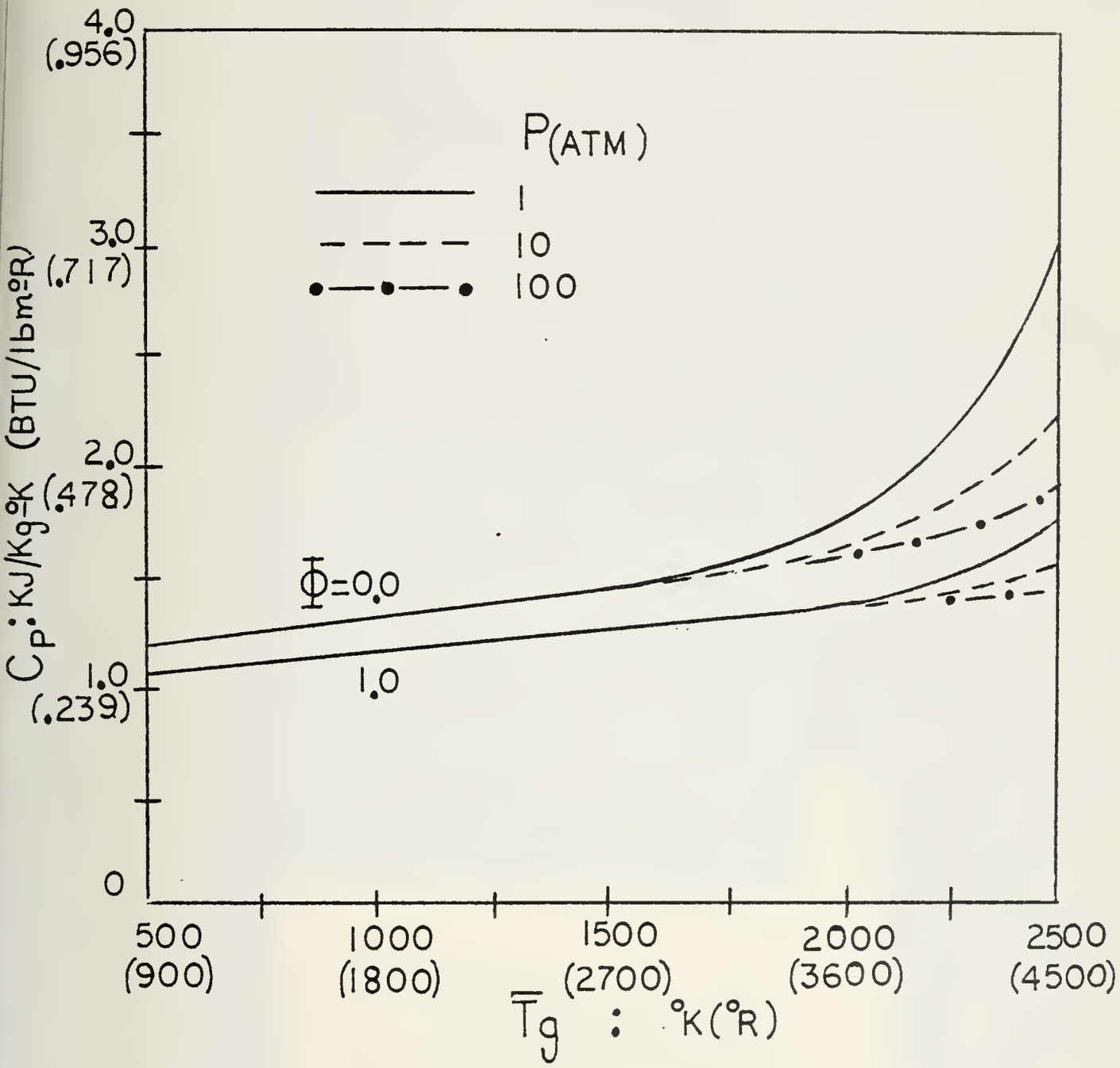

FIGURE C-2: C_p of lean hydrocarbon-air combustion products as a function of P, $\bar{T}g$, and Φ; fuel C_nH_{2n} [7]

Thesis
207072
J8245 Jorgensen
Predicted heat transfer loss in the expansion cylinder of a two cylinder cycle reciprocating engine.